Dielectric Properties of

$Cu_{0.5}\ Tl_{0.5}\ Ba_2\ Ca_2\ Cu_{3-x}\ M_x\ O_{10-\delta}$

$(M = Cd, Zn, Ni : x = 0, 1.5)$ Superconductors.

Diss
PHY
1191
ا-ب

Aisha Saba

Department of Physics

Quaid-i-Azam University

Islamabad,

2017

Diss
PHY
1191
C-1

Dielectric Properties of

$Cu_{0.5}Tl_{0.5}Ba_2Ca_2Cu_{3-x}M_xO_{10-\delta}$

$(M = Cd, Zn, Ni : x = 0, 1.5)$ Superconductors.

A dissertation submitted to the department of physics, Quaid-I-Azam University, Islamabad, in the partial fulfilment of the requirement for the degree of

Master of Philosophy
in
Physics
By

Aisha Saba

ومن يُؤت الحكمة فقد أُوتي خيرًا كثيرًا

QUAID-I-AZAM UNIVERSITY
ISLAMABAD

Material Science Laboratory
Department of Physics
Quaid-I-Azam University
Islamabad, Pakistan

2017

شروع اللہ رحمن اور رحیم۔ اور ہم سب کے درمیان سب سے زیادہ خود مختار کے نام کے ساتھ۔

Beginning with the name of ALLAH, The Most Beneficent and The Merciful.

Certificate

This is to certify that Ms. Aisha Saba D/O Muhammad Aslam has carried out the experimental work in this dissertation under my supervision in Materials Science Laboratory, Department of Physics, Quaid-i-Azam University, Islamabad and satisfying the dissertation requirement for the degree of Master of Philosophy in Physics.

Supervisor

Dr. Nawazish Ali Khan
Department of Physics
Quaid-i-Azam University
Islamabad, Pakistan.

Submitted through

Chairman

Prof. Dr. Arif Mumtaz
Department of Physics
Quaid-I-Azam University Islamabad, Pakistan.

DEDICATED

TO

My Hero Father, Supportive Mother, Caring Brothers and Loving Sister.

ACKNOWLEDGEMENTS

All the praises to Almighty ALLAH, the most merciful and the sovereign power, who made me able to accomplish this research work successfully. I offer my humble and sincere words of thanks to his Holy Prophet Muhammad (P.B.U.H) who is forever a source of guidance and knowledge for humanity.

This work would have not been possible without the invaluable contributions of many individuals. First and foremost, I wish to thank my supervisor Dr. Nawazish Ali Khan for all of his support, advice, and guidance during the whole period of my study. I am thankful to chairman, department of physics, for the provision of all possible facilities and cooperation. I would like to thank to all my seniors and juniors, Asad Raza, Abida Saleem, Syed Hamza Safeer, Muhammad Hassan, Farwa Ali and Muhammad Ibrahim for technical guidance and support.

My humble and heartfelt gratitude is reserved for my beloved Parents, sister and brothers. Without their prayers, support and encouragement the completion of this study task would have been a dream.

Aisha Saba

Abstract:

We have synthesized $Cu_{0.5}Tl_{0.5}Ba_2$ $Ca_2Cu_3O_{10-\delta}$ and $Cu_{0.5}Tl_{0.5}Ba_2$ $Ca_2Cu_{1.5}O_{10-\delta}$ (M=Cd, Zn, Ni) superconducting samples. The samples were synthesized by two step solid state reaction method. We have studied dielectric properties of these samples at low frequency. The main objectives of these studies were to investigate the role of Cd, Zn, and Ni doping in our superconductors (HTSC). We have measured dielectric constants (ε' and ε''), dielectric loss ($\tan\delta$) and ac conductivity (σ_{ac}). In the resistivity measurements these samples have shown metallic variations of resistivity from room temperature down to onset of superconductivity. The onset of superconductivity in $Cu_{0.5}Tl_{0.5}Ba_2$ $Ca_2Cu_3O_{10-\delta}$ and $Cu_{0.5}Tl_{0.5}Ba_2$ $Ca_2Cu_{1.5}M_{1.5}O_{10-\delta}$ (M=Cd, Zn, Ni) samples are observed at 105.6, 101.7, 114, 106.3K and T_c (R=0) at 98.3, 95.4, 102.3, 102K respectively. The negative capacitance is observed in our $Cu_{0.5}Tl_{0.5}Ba_2$ $Ca_2Cu_3O_{10-\delta}$ and $Cu_{0.5}Tl_{0.5}Ba_2$ $Ca_2Cu_{1.5}O_{10-\delta}$ (M=Cd, Zn, Ni) superconducting samples.We observed that dielectric properties of $Cu_{0.5}Tl_{0.5}Ba_2$ $Ca_2Cu_3O_{10-\delta}$ and $Cu_{0.5}Tl_{0.5}Ba_2$ $Ca_2Cu_{1.5}O_{10-\delta}$ (M=Cd, Zn, Ni) superconducting samples depends on temperature and frequency of electric field.

Figures of Content

Tables of Contents

Chapter # 1
Introduction to Superconductivity

1.1 Superconductivity:

The phenomenon of superconductivity, in which electric resistance of many materials completely disappears and expulsion of magnetic field lines occurring in certain materials at low temperature, was discovered by Heike Kimerling Onnes and one of his assistant on April 8,1911 in Leiden [1].

Kamerlingh Onnes examined that at certain temperature about 4 K, the resistivity of Mercury (Hg) was zero which means that at the critical temperature the resistance was immediately dropped to zero. It was a miracle discovery and is one of the most fascinating and revolutionary branch in condense matter physics.

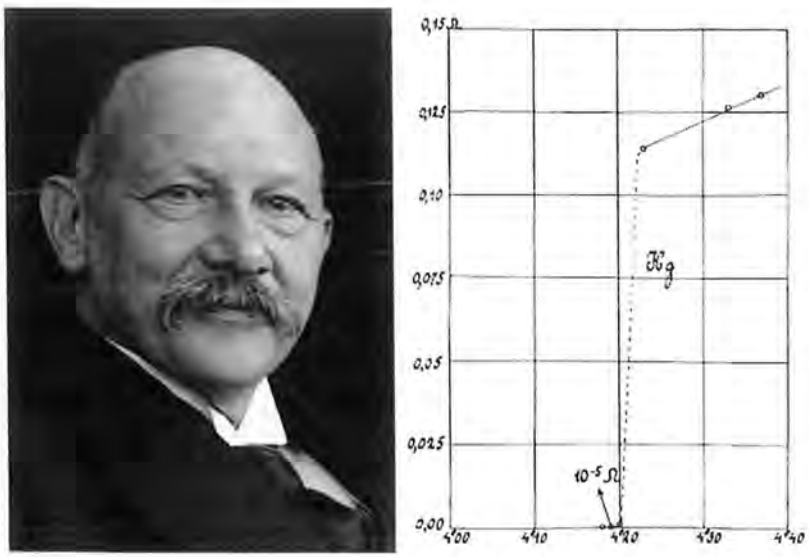

Fig 1.1. Experimental data obtained in mercury by H. Kamerlingh Onnes in 1911, showing for the first time the transition from the normal state to the superconducting state.

1.2 Vital properties of superconductors:

Superconductivity [2] is defined by the following properties

- Zero resistivity
- Perfect diamagnetism

- **1.2.1. Zero Resistivity:**
  Resistance is the hurdle to the flow of electron. In normal state, an electron makes countless collisions with fixed atoms, transfers its energy to the lattice atoms which vibrates and loses energy in the form of heat. As a result, energy keeps on dissipating. The resistivity (**ρ**) is defined as

$$\sigma = ne^2\frac{\tau}{m} \quad \ldots\ldots\ldots\ldots\ldots (1.1)$$

$$\rho = \frac{1}{\sigma}$$

$$\rho = \frac{m}{n\tau e^2} \quad \ldots\ldots\ldots\ldots\ldots (1.2)$$

Where m is mass of electron, τ is mean free time, e is charge on an electron and n is number density of electrons. By slowly cooling the sample, the lattice vibrations start to freeze. As a result, electron-lattice vibrations diminishes. Therefore, for infinite mean free time, the electrical resistivity vanishes completely in superconductors at certain low temperature. So in superconducting state, a pair of electrons bounds together via phonons and this pair is called cooper's pair. This cooper's pair can flow without energy dissipation.

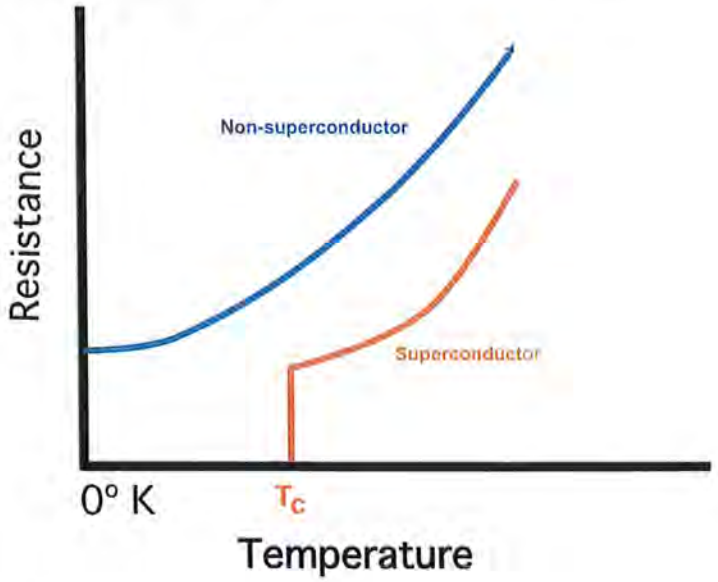

Fig 1.2: Resistance vs Temperature curve for superconductor.

1.2.2. Perfect Diamagnetism or Meissner's Effect:

When we place diamagnetic materials in an external magnetic field, these materials create an induced magnetic field in opposite direction and their magnetic moments align themselves in such a way that they oppose the external magnetic field as shown in fig. 1.3. This phenomenon is known as diamagnetism.

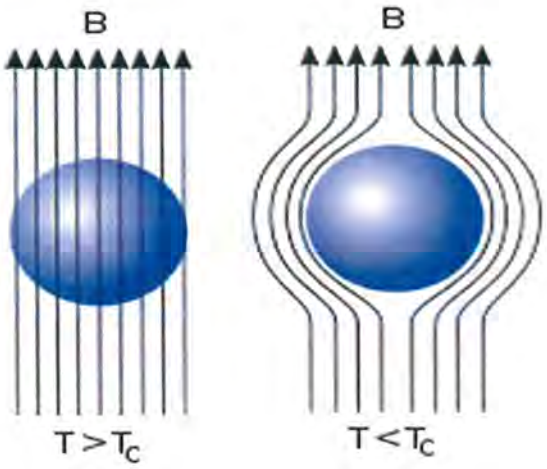

Fig. 1.3: Meissner's effect in a material.

In 1933, Meissner and Ochsenfeld observed that when they placed a superconducting sample in external magnetic field, the magnetic flux is expelled from their sample. This is known as Meissner's Effect and the superconductors shows diamagnetism response. The Meissner's Effect is the contrary phenomenon [4].

Since,

$$B = \mu_o(H + M) \quad \ldots\ldots\ldots\ldots \textbf{(1.3)}$$

As the magnetic field disappears in the superconductor so B = 0

$$0 = \mu_o(H + M)$$

$$M = -H$$

Therefore, the susceptibility is

$$\frac{M}{H} = \chi = -1$$

$$\chi = -1 \quad \ldots\ldots\ldots\ldots\ldots \textbf{(1.4)}$$

This is the susceptibility of perfect diamagnetic substance, so superconductors show perfect diamagnetism.

1.3 Parameters of Superconducting state:

For superconductivity, in a given sample three critical values i.e. critical temperature (T_c), critical current density (J_c) and critical magnetic field (H_c) are essential. For a sample exhibiting superconductivity, these parameters must be less than their critical values.

1.3.1 Critical temperature (T_c):

At room temperature (290K), the superconducting material is in normal state and there is current dissipation due to electrical resistivity (collision of electrons with atoms). Nevertheless, when the superconductor cooled down below some temperature the electrical resistivity of a superconductor rapidly disappears and this state of the material is defined as superconducting state. The temperature at which, the electrical resistivity of a superconductor rapidly drops to zero, is known as critical temperature 'T_c'. There is reasonable resistivity above the critical temperature and resistivity vanishes at below the critical temperature. Different superconducting materials have different critical temperatures as given in the following table 1.1.

Materials	Critical temperature T_c (K)
Hg	4.2
C_6Ca	11.5
V_3Si	17.1
Nb_3Sn	18.3
$TlSrLaCuO_5$	40
$YBa_2Cu_3O_7$	90
$Tl_2Ba_2Ca_2Cu_3O_{10}$	125

Table 1.1: Critical temperature of superconducting materials

1.3.2 Critical current density (J_c):

Relatively thin wires of superconductors are used for large currents because there is small or no resistance. Nevertheless, there is a limit of current to flow through these thin wires. So, the maximum current per unit cross sectional area flowing through the superconductor, above which sample becomes normal state, is known as Critical current density 'J_c'. In 1961, Kunzler was first physicist who observed this [5]. Critical current density (J_c) depends on temperature.

For practical uses, the critical current density (J_c) value must be greater than 1000 amperes per square millimetre (A/mm^2). While in Thallium based superconductors, we can achieve up to 10^6 to 10^7 (A/cm^2) at very low temperature (5 K).

1.3.3 Critical magnetic field (H_c):

The superconductivity not only ruined by the increasing of temperature above its critical value but it can also be destroyed by increasing the external magnetic field. The external field at which the superconductivity destroyed is called critical magnetic field. This was first observed by Meissner when he was studying the behaviour of superconductors at different magnetic field and he observed that after certain value of external field, superconductor will be in normal state. Figure.1.4

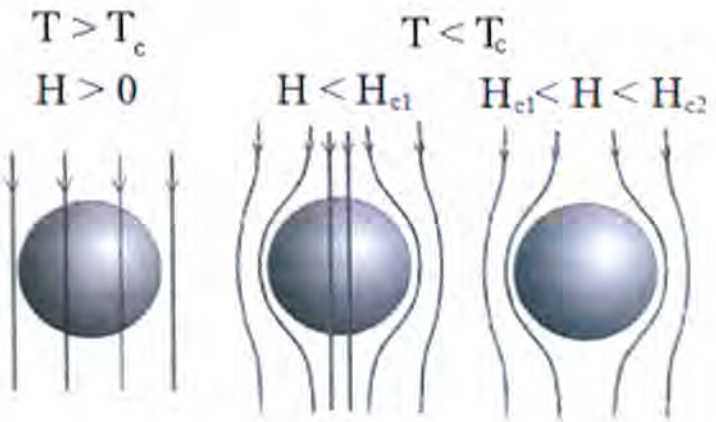

Figure 1.4: Meissner effect.

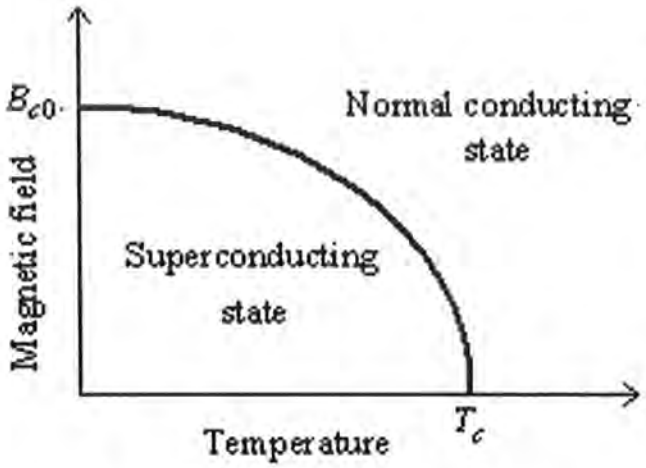

Figure 1.5: critical magnetic field as a function of temperature.

Fig 1.5 shows that the critical magnetic field is function of temperature. It slowly decreases when temperature increases from T= 0 K to T=T_c. The relation given below, defines the variation of critical magnetic field H_c with temperature

$$H_c(T) = H_c(0)\,[1-(T/T_c)] \quad \text{.....(1.5)}$$

Where H_c (0) is maximum value of magnetic field at 0 K and at T=T_C, H_C (T_C) = 0. We can also measure the value of critical current 'I'_c using the given relation,

$$I_c = 2\pi r H \quad \text{..... (1.6)}$$

1.4. Types of Superconductors:

Vitaly Lazarevich Ginzburg and Lev landau proposed the idea of two kinds of superconducting samples in their paper **[6]**. In the start, all superconductors were considered as type I but with the passage of time, the scientist name Lev Shubnikov, observed that there are some superconducting samples behaved differently in response to external magnetic fields. He named them as type II superconductors. Later on, Alexei Alexeyich Abrihosov developed the theory for type-II superconductors and Nobel Prize was awarded him for his revolutionary work [7]. One can easily decide whether the material is a Type- I or Type-II superconductor based on response of magnetic field.

1.4.1. Type-I Superconductor:

Type I superconductors have low critical temperature and sudden transition from normal state to superconducting state in magnetic field. Type I superconductors are soft superconductors. They are composed of alloys and pure elements; they also have low critical magnetic field. The maximum critical magnetic field is 0.2 *T*

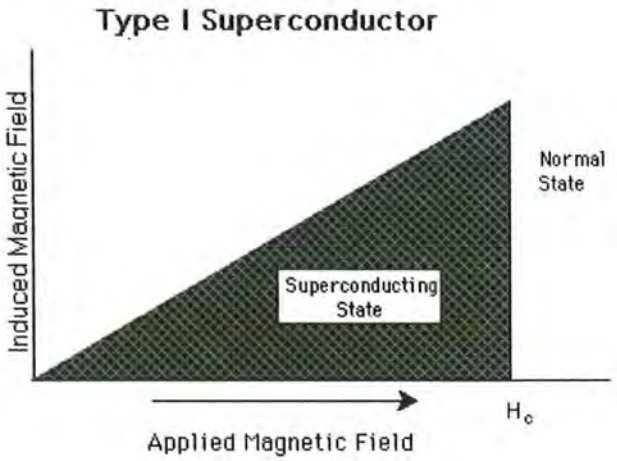

Fig 1.6: Type-I Superconductor.

1.4.2. Type-II Superconductor:

These superconductors are hard superconductors. They contain alloys or transition metals. They have high value of resistivity in applied magnetic field than type I superconductors [8]. Type II superconducting samples slowly changes from normal state to superconducting state, in other words they do not show sudden transition.

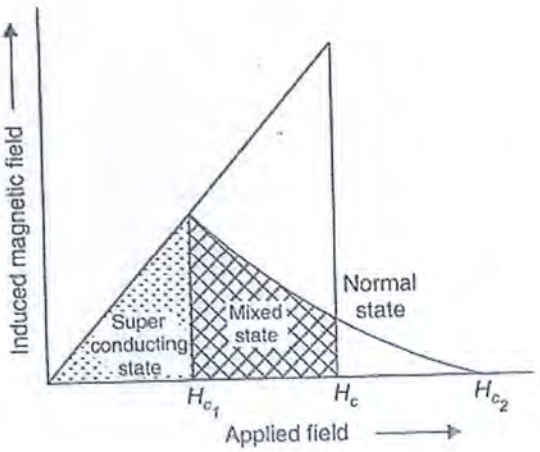

Fig 1.7: Type-II Superconductor

From figure 1.7, for region $H < H_{c1}$ no magnetic flux can penetrate in the bulk of the sample, this region is a perfect diamagnetic, H_{c1} is known as "**lower critical field**". Further increase in magnetic field, superconducting sample can transform to mixed state in which the sample have both states (normal and superconducting). The region where $H_{c1} < H < H_{c2}$ known as

intermediate or mixed state region or vortex region. The region $H > H_{c2}$ where magnetic flux can penetrate in and is called paramagnetic state and sample is in normal state.

1.5.Evolution of theory of superconductivity:

After the discovery of superconductivity, different scientists were working on the theory of superconductivity and many theories were given to explain the phenomenon of superconductivity. In 1935, the two brothers Heinz and Fritz London gave the very first phenomenological theory. Their theory was based on two fluid model. Another theory was given by V.L. Ginzburg and L.D. Landau, it was the very first quantum theory to describe superconductivity, in which they used wave function "ψ" as an order parameter. In 1957, the first microscopic theory of superconductivity known as BCS(Bardeen-Cooper-Schrrieffer) theory, given by John Bardeen, Leon Neil Cooper and John Robert Schrieffer.

1.5.1 London theory:

In 1935, two brothers Heinz and Fritz London developed a theory to describe the Meissner's effect. They used two fluid model, they divided all the electrons of superconducting samples into two types; normal electrons " n_n " and superconducting electrons " n_s", so total density is n= $n_s + n_n$ .As temperature approaches to critical temperature ($T \to Tc$), the number of superconducting electrons would be maximum.

$$T \to Tc, n_n \to 0 \ so \ n_s \to \max for (T<Tc)$$

And $$T \to Tc, n_s \to 0 \ so \ n_n \to \max as \ for (T>Tc)$$

Consider the uniform electromagnetic field applied on the superconducting sample. We assume that both fields are so weak, so they do not impact with the superconducting electrons. If V_s is the average velocity, m is the mass and e is the charge of the super electron, then in the presence of field E the equation of motion, is

$$m (d v_s/d t) = -e E \quad \ldots\ldots\ldots\ldots\ldots\ldots (1.7)$$

The current density of superconducting electron is by

$$J_S = -e n_s V_s \quad \ldots\ldots\ldots\ldots\ldots\ldots (1.8)$$

From question 1.7 and 1.8 we have

$$dJ_s/dt = (n_s e^2/m)\, E \quad \ldots\ldots\ldots\ldots\ldots \quad (1.9)$$

Which is known as first London equation and this shows that in the absence of an electric field, steady state current J_S is constant.

On the other hand, the current density of the normal electrons is $J_n = \sigma E$. Shows that E=0, typical behaviour of normal state.

The Maxwell equation is,

$$\nabla \times E = -\, dB/d\,t \quad \ldots\ldots\ldots\ldots\ldots \quad (1.10)$$

As E=0 i.e. B = constant which shows that magnetic field is uniform inside the superconductor, which is in contradiction with the Meissner's effect.

To remove this difference, London suggested some adjustment in the expression [9], which is

$$\nabla \times J_s = -\frac{n_s e^2}{m} B \quad \ldots\ldots\ldots\ldots\ldots \quad (1.11)$$

Known as London second equation and result is in agreement with the experiment.

1.5.1.1 London penetration depth:

When we apply magnetic field lines at the surface of a superconductor, magnetic field lines can penetrate into the superconductor to the length called London penetration depth denoted as λ_L, which decays exponentially.

Using Maxwell's equation,

$$\nabla \times B = \mu_o J_s \quad \ldots\ldots\ldots\ldots\ldots \quad (1.12)$$

By taking curl and using 1.11,

$$\nabla \times (\nabla \times B) = -\frac{\mu_o n_s e^2}{m} B = -\frac{1}{\lambda^2} B \ldots\ldots\ldots\ldots\ldots \quad (1.13)$$

where

$$\lambda_L = (m_e/\mu_o n_s e^2)^{1/2}$$

is London penetration depth.

As $\nabla \times (\nabla \times B) = \nabla (\nabla . B) - \nabla^2 B$

And as we know

$$(\nabla . B) = 0$$

So, equation 1.12 becomes,

$$\nabla^2 B = \frac{1}{\lambda^2} B$$

For 1-d, solution is

$$B = B_o e^{-x/\lambda_L} \quad \text{..... (1.14)}$$

And $\mathbf{B_o}$ is externally applied field and values of λ_L varies from 50nm to 500nm.

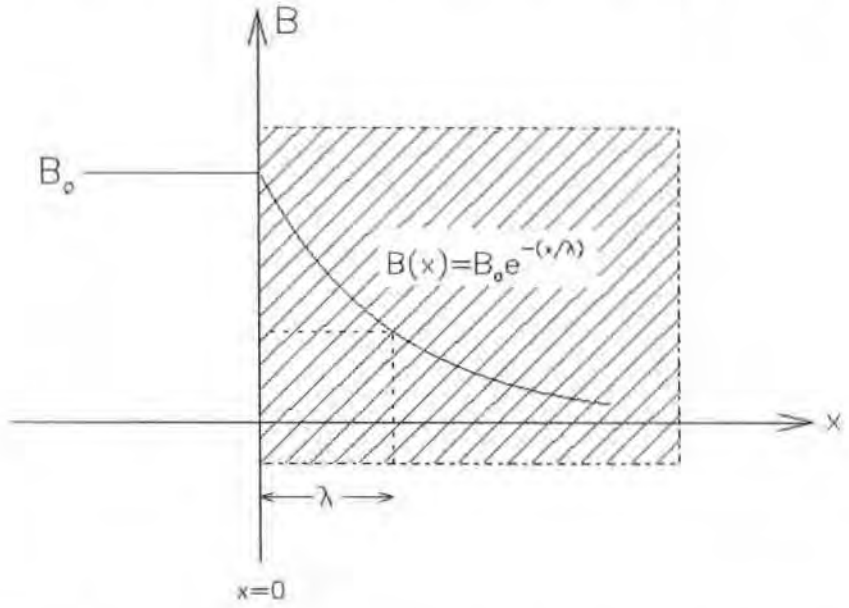

Fig. 1.8: Decay of magnetic field inside the superconducing material.

London penetration depth also depends on the temperature. The penetration depth decreases with increasing temperature and relation is [10],

$$\lambda(T) = \frac{\lambda(0)}{[1+(\frac{T}{T_c})^4]^{1/2}} \quad \text{..... (1.15)}$$

and $\lambda(0)$ is penetration depth at zero Kelvin temperature.

1.5.2. Ginzburg-Landau Theory:

In 1950, V.L. Ginzburg and L.D. Landau proposed a first quantum theory of superconductivity which is called GL theory. They used a wave function, which depends on

spatial part, denoted as ψ. They claimed about the existence of an order parameter [11] and according to them, this order parameter is zero in the normal state or above the critical temperature T_C whereas it is non-zero for superconducting state or below the critical temperature T_c i.e.

$$\Psi(T) = 0 \quad ; \text{If} \qquad T > T_c$$

$$\Psi(T) \neq 0 \quad ; \text{If} \qquad T < T_c$$

so basically it suggests about the state of a system.

GL theory explained that wave function Ψ should be a complex number. It is a macroscopic wave function for a superconductor. When they were working originally on the signification of Ψ, they were not much clear about it.

1.5.3. BCS theory:

In 1957, the scientists Bardeen, Cooper and Schrieffer [12] presented a first quantum mechanical theory of superconductivity, known as BCS theory. This theory is based on advance quantum mechanical concepts. Their theory defines superconductivity as a microscopic effect due to condensation of cooper pair.

1.5.3.1. Formation of Cooper pairs:

According to BCS theory, when electrons pass through the perfectly arranged positive ions, they produce deformation in the crystal lattice.

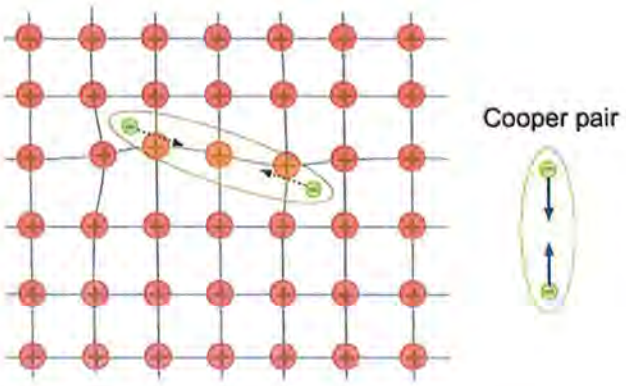

Fig. 1.9: Lattice of a superconductor and formation of Cooper pair.

As a result, atoms of lattice vibrates and these vibrations are known as phonons. In a metal, an electron moves freely, repelled from other electrons due to same charges but they attract the ions and this attraction deforms lattice. As ions attracted towards an electron and offer more positive charge to the electron to form a positive ion core. This greater positively charged ion core attracts other electron of opposite momentum and spin [13]. As electrons are fermions, but their total spin is zero like bosons. Many Cooper pairs can be in same state. This pair of electrons known as Cooper pair. The Cooper pair is main reason for superconductivity.

1.5.3.2 Coherence Length (ξ):

In cooper pair, electrons are not necessarily close, they may be far apart because their interaction has long range, may be of few hundred nanometers. There is some distance between them [14] and this distance between them is known as coherence length (ξ). In high temperature superconductors, it is small and in case of low temperature superconductors its value is large. According to BCS theory, the coherence length is,

$$\xi = \frac{\hbar V_F}{2\Delta}$$

Where V_F is he Fermi Velocity and 2Δ is the energy gap.

For type I superconductors: $\xi > \lambda_L$

For type II superconductors: $\xi < \lambda_L$

1.6 The Isotope effect:

This effect shows that critical temperature varies with different mass of isotopes of superconducting elements [15- 17], and relation is given by,

$$T_C \propto M^{-\alpha}$$

Or

$$M^{\alpha} T_c = \text{constant} \quad \ldots\ldots\ldots\ldots\ldots\ldots \textbf{(1.16)}$$

Where α is fitting constant and its value is 1/2.

1.7 Josephson Effect:

In 1962, the phenomenon of supercurrent across Josephson junction was predicted by Barian David Josephson. This effect is macroscopic quantum mechanical tunneling

phenomenon. He explained that as current flows through a thin (order of a few nanometers) insulating barrier between two superconductors (Josephson junction), cooper pairs tunnel through insulator barrier [18,19]. Their tunneling through insulating barrier called Josephson Effect. The Josephson Effect has two types,

- Dc Josephson effect
- Ac Josephson effect.

1.7.1 Dc Josephson effect:

The flow of Cooper pairs is supercurrent. It flows indefinitely without external voltage. It was Josephson who predicted that two superconductors, which are separated by a thin insulator then quantum tunneling may happen for Cooper pairs. The wave function of the Cooper pairs penetrates into the insulating layer and sealed together in phase. So supercurrent can flow through insulating layer in the absence of externally applied voltage, and that is DC Josephson effect.

1.7.2 Ac Josephson effect:

If we irradiate the junction with current of frequency ω, we will get a different effect then DC Josephson effect. The flow of current (with amplitude and frequency) during quantum tunnelling of Cooper pairs across the insulating layer at a fixed voltage, is sustained across a tunnel barrier is known as the ac Josephson Effect.

1.8 Dielectric properties of Superconducting samples:

The dielectric property that we analysed is permittivity and we know permittivity is not constant. It can change with temperature, frequency, pressure and structure of sample.

1.8.1 Capacitor:

Capacitor is a single or multi layered electronic device, to store charge in electric field. It consists of different layers of conductor and dielectric. To make our capacitor we painted both sides of samples with silver paste.

1.8.2 Dielectric constant:

A material is considered as dielectric if it has the capacity to store energy when an electric field is applied. When a voltage is applied across a parallel plate capacitor its begin to charge,

and more quantity of charge is stored when a dielectric material is placed between the plates than if there is no material is between the plates. So the dielectric material increases the storage capacity of the capacitor by, which usually would contribute to the field. The capacitance of a capacitor with dielectric material is associated to dielectric constant.

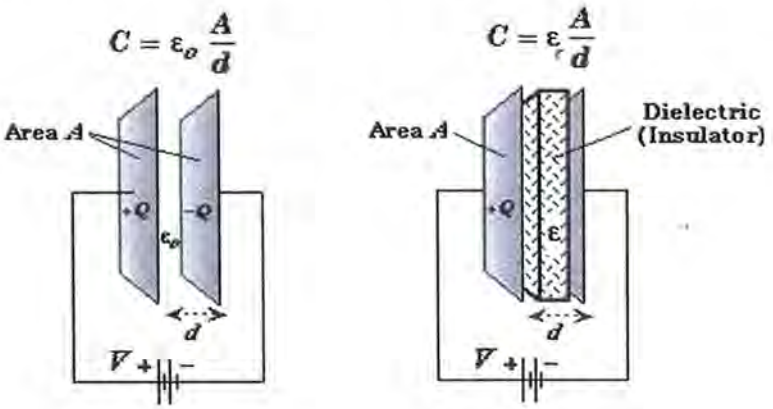

Fig. 1.10: Capacitors with and without dielectric material.

ε is the permittivity or dielectric constant of material, and A is the area of plates and d is the distance between them.

The complex dielectric constant ε contains of a real part ε′ which indicates the storage and its imaginary part ε″ which indicates the loss. Using the electromagnetic theory, the definition of electric flux density (electric displacement) D_f is:

$$D_f = \varepsilon E$$

As $\varepsilon = \varepsilon_0 \varepsilon_r$ is the permittivity and ε_r is the relative permittivity. Permittivity is a complex quantity and explains the interaction of a substance with field E.

Dielectric constant (ε) is equal to relative permittivity (ε_r) relative to the free space permittivity (ε_0.). The real part of permittivity (ε_r') is estimate that how much energy from an external field is stored in a material. The imaginary part of permittivity (ε_r''), is a measure of how dissipative a material is to an external electric field, is called the loss factor. The imaginary part of permittivity (ε_r'') is generally much lesser than ε_r' but always greater than zero and the loss factor contains the properties of both dielectric loss and conductivity.

1.8.3 Dielectric loss:

The dielectric loss or tangent loss 'tanδ' defined as the ratio of the imaginary part to the real part of the dielectric constant.

$$\tan\delta = \varepsilon_r''/\varepsilon_r' \quad \ldots\ldots\ldots\ldots\ldots\ldots \quad (1.17)$$

It is also known as tan delta or dissipation factor.

1.9 Technological applications of superconductors:

Superconductivity is revolutionary field. Superconductors are very efficient conductors, superconductors are being used by engineers and scientists in the field of research and industry in the whole world. Some of the applications are,

1.9.1 In the field of medical:

- Magnetic Resonance Image (MRI)
- Biotechnical engineering

1.9.2 Electronic devices:

- Particle accelerators
- Particle Colliders (Synchrotrons and Cyclotrons)
- Josephson junction devices
- Sensors
- Transistors

1.9.3 Industrial:

- Superconducting magnetic
- Magnetic shielding
- Sensors

1.9.4 Transportation:

- magnetic levitation trains
- superconducting marine propulsion

1.9.5 Power generators:

- Superconducting transmission lines
- Energy storage
- Transformers
- Superconducting generators

References:

[1]. R. Simon and A. Smith: Superconductors: Conquering Technology's New Frontier (Plenum, New York, 1988).

[2]. K. Fossheim and A. Sudbo: Superconductivity-Physics and Applications, John Willey and Sons Ltd. 2005

[3]. S. O. Pillai, Solid state physics, 5th ed

[4]. Solid state physics and Electronics R.K Puri and V.K Babbar, 278(1997)

[5]. J. E. Kunzler, E. Buehler, F. S. L. Hsu and J. H. Wernick: Physical Review Letters 6 (3), (1961) 89-91.

[6]. V. L. Ginzburg and L. D. Landau: Zh. Eksp. Teor. Fiz 20, (1950) 1064.

[7]. A. Abrikosov: Zh. Eksp. Teor. Fiz 32, (1957) 1442.

[8]. V.V. Schmidt, (Eds) P. Muller, A.V. Ostinov: the Physics of Superconductors, (1997).

[9]. F. London, H. London: Proc. Roy. Soc A149, 71

[10]. V. V. Smith book

[11]. P. Mandal, A.Poddar, A.N. Das, B.Ghosh, P.Choudhary: Physica C, 169 (1990) 43-49.

[12]. J. Bardeen, L. N. Cooper and J. R. Schrieffer: Physical Review ,106 (1), (1957) 162-164.

[13]. H. Ibach and H. Lüth, Solid-State Physics: An Introduction to Principles of Materials Science (2009).

[14]. S.O.Pillai, Solid State Physics, 5th Edition, New Age International (p) Limited Publishers (2002).

[15]. H. Froehlich,: Physical Review, 79 (1950) 845-856.

[16]. K. Conder, Materials Science and Engineering: R: Reports 32 (2–3), (2001) 41-102.

[17]. G. Sorensen and S. Gygax,: Physical Review, B 51 (17), (1995) 11848-11859.

[18].Josephson, B. D., "Possible new effects in superconductive tunnelling," Physics Letters 1(1962) 251.

[19]. Josephson, B. D.: Rev. Mod. Phys. 46 (2) (1974)251–254.

Chapter # 2

Literature Review

2.1 Review of Thallium based Superconductors:

Z. Z. Sheng et al. [1], discovered the superconductivity in thallium cuprates for the very first time. They claimed that their samples were stale, reproducible and have high critical temperature (above 100K). Their thallium based superconductors have zero resistance above 100K. Before them many scientists were working on high temperature superconductors but their superconductors were unstable and irreproducible. By using Tl-Ca-Ba-Cu-O superconductors, they improved critical temperature and the values of critical temperature for their samples, were much higher than many other rare earth contain superconductors.

L.Perez. Arrieta et al [2], performed two stepped process to prepared their superconducting samples $TlBa_2Ca_2Cu_3O_x$ and analysed their behaviour. To prepare samples, they utilized a two stage furnace by different thallium diffusion at 823K (550^0C) and used spray pyrolysis techniques to deposit films of samples. So the precursors of samples were formed. Then they placed samples in different flow rates of oxygen, added different quantity of thallium oxide, pressure was generated to get the pressure of thallium oxide which was ranging from 6.9 $\times 10^{-4}$ to 6.1×10^{-2} atm 750°C. So They made their films with c-axis perpendicular to the surface of substrate. As the samples have mixture of two materials ($BaCuO_2$ and $Tl-1223$), they got crystalline grains with large side with superconducting behaviour was better for a thallium oxide pressure of 1.4×10^{-2}atm. For their films the critical temperature T_c values were from 90K to 120K.

Najmul Hassan et al. [3], reported the structure and properties of superconducting samples $Cu_{0.5}Tl_{0.5}Ba_2Ca_{0.5}M_{1.5}Cu_{1.5}Ni_{1.5}O_{10-\delta}$ (M=Mg, Be). To prepared the precursor of their samples they used the solid-state reaction technique and characterized their superconducting samples by resistivity, x-ray diffraction, ac- susceptibility and FTIR. Using X-ray diffraction, they analyzed that as they increased the concentration of doping, the length of c- axis of unit cell of the samples decreases. As the doping atoms have a small ionic size so the decrease in c-axis. They reported that from resistivity and susceptibility behaviour of doped samples, critical temperature T_c increases. They explained this phenomenon as inter-plane coupling, so more electrically negative atoms of doping at Ca sites. The neighboring NiO_2/CuO_2 planes help the carriers to raise inter- plane coupling. They also observed the coherence length along c-axis increased and the anisotropy lowers. From the FTIR, the oxygen modes were start shifted towards the low wave number. The magnitude of diamagnetism was decrease due to increase in the coherence length and low anisotropy in the superconducting sample.

S. Isber et al. [4], manufactured the superconducting samples of $TlBa_2Ca_2$ $(Cu_{3-x}$ $CO_x)$ $O_{9-\delta}$ with (x=0-0.6), using the single step solid-state reaction. To characterize their superconducting samples, they used x-ray powder diffraction, resistivity and susceptibility. Using XRD analysis, they explained that their superconducting samples have tetragonal structure and discovered different parameters of unit cell. From resistivity and susceptibility measurements, they came to know that the critical temperature T_c suppressed with the doping of CO at copper oxide planes. To explain the suppression in T_c, they took the help of Abrikosov and Grokov model and the realized that the reason behind the suppression in Temperature was cooper pair- breaking phenomenon. They told that with the doping of the CO, the reversibility field and critical current density J_c decreases. And they also came to know that the inter-grain junctions have Superconductor-normal-superconductor type.

Nawazish A. Khan et al. [5], created the superconductors $TlBa_2$ $(Ca_{3-y}$ $M_y)$ Cu_4 $O_{12-\delta}$ (M=Be; y=0, 0.5, 1.0, 1.5, 2) and characterized their samples using different apparatuses and methods, i.e. XRD, FTIR, resistivity and ac-susceptibility measurements. From XRD, they explained that their samples have tetragonal structure. They described that by increasing the doping, the volume of the unit cell increases and c-axis length decreases. They realized that the superconductivity suppressed as they increased doping. They performed FTIR and observed that the planer oxygen and apical oxygen modes slanted towards the low wave numbers, which was the vivid indication of inter-plane coupling improved. When they placed their samples in O_2 for annealing, the value of diamagnetism suppresses. At the end, the oxygen reduces the carrier concentration in the cell. So, superconductivity suppresses. They explained that anti ferromagnetic alignments which occurs in the CuO_2 planes suppress due to doped atoms of Be, superconductivity increases. The real purpose to synthesize their samples $TlBa_2$ $(Ca_{3-y}$ $M_y)$ Cu_4 $O_{12-\delta}$ (M=Be; y=0, 0.5, 1.0, 1.5, 2) was to boost the inter-plane coupling and reduction of anti-ferromagnetic alignment. The inter plane coupling can be attained by high electro-negativity and doping with such atoms which have small to Ca atom. As they doped Be atom which has small size to Ca atom. The boosted inter plane-coupling roots to reduce the amount of anti-ferromagnetic in the CuO_2 planes.

A. Iyo et al. [6], worked on the superconductors $TlBa_2Ca_{n-1}Cu_nO_y$ (n=3 and n=4). The precursor was synthesized using the solid-state reaction technique. It is impossible to eliminate the Corban contents totally from precursor because they have used Ba (NO_3),

$Ca(NO_3)_2$ and CuO. Therefore, precursor consists of a small concentration of carbon and cause to defeat the superconductivity. They explained this phenomenon as, when residual carbon atoms entered into the thallium atoms, it reduced the concentration of holes in copper oxide planes which added impurities in material and that is not suitable for the formation of ideal composition. They performed X-ray diffraction, composition analysis and susceptibility analysis for characterization. They observed that by changing the different parameters, the superconductivity has changed. They concluded by increasing the pressure, the critical temperature T_c increases. They also observed that if quantity of thallium decreases, the T_c of superconductor Tl 1234 also increases. They also reported that critical temperature T_c was improved by adding thallium. They achieved maximum transition temperature Tc, for superconducting samples Tl Ba_2 Ca_{n-1} Cu_n O_y was 133.5 K and 127 K for n =3 and n= 4 respectively.

Nawazish A. Khan et al. [7], prepared superconducting samples $(Cu_{0.5}Tl_{0.5})$ Ba_2Ca_2 $(Cu_{3-x}Ti_x)$ $O_{10-\delta}$ (x = 0, 0.25, 0.50, 0.75). To synthesize their samples, they used the solid-state reaction technique at 860° C. They studied the properties of samples by using X-ray scans, resistivity, ac-susceptibility and FTIR. From resistivity analysis, they described that samples showed that the T_c decreased by doping of Titanium and their samples had orthorhombic structure with PMMM space group. They calculated the parameters of the unit cell which were doped with Titanium atoms at the Cu planes, the length of c-axis and the orthorhombic distortion increases and they suggest that increase in orthorhombic distortion was because of the different ionic radii i.e. 0.90 Å and 0.69 Å for titanium and copper respectively. Their Fourier Transform Infrared Spectroscopy (FTIR) results indicated that planer oxygen modes have shifted towards the high wave numbers which means they were toughened as the doping was increased. And this toughening of planer oxygen modes was because of the lager ionic radius and the smaller mass as compared to Copper atom. As atoms with low mass vibrates at higher frequencies. Thus, oscillations were produced due to Titanium atoms at Cu sites would be harmonic and it reduces the density of phonon population $g(\omega)$. As $g(\omega) = (N\tau/2\pi^2v^3)\,\omega^2$ and $\omega = qv$

Where,

N is the number of primitive cells, τ = volume of the unit cell.

We know superconductivity lies in CuO planes, from the above expression if the volume

decreases than g(ω) also decreases which leads to reduction in phonon-electron interaction, weknow electron-phonon interaction is necessary for superconductivity.

Y. Shimakava et al [8], worked on $Tl_2Ba_2CaO_6$ samples. They examined the structure of crystal, transition temperature (T_c) and carrier concentration in their superconducting samples. They perceived that values of critical temperature (T_c) of their samples, are related with c – axis length, according to them the variation in the transition temperature is because of small variation in oxygen content, so they proved that transition temperature (T_c) depends on carrier concentration. They also realized that critical temperature (T_c) might be grow about at 80K and length of c – axis might be lengthening 0.4% by increasing oxygen about 0.1 per formula. They expressed that critical temperature T_c suppress when they increased quantity of dopant. They concluded that in their samples, as they increased hole's concentration it suppressed the superconductivity and when they decrease hole's concentration it boosted their superconductivity. They described that when they increase number sheet of CuO_2 per unit formula, there was variation in transition temperature. As they increased it (CuO_2) then concentration carrier number per sheet became less. They noted that only for some appropriate range of carrier concentration, the superconductivity exists.

Nae. Lih. Wu et al [9], they discovered a new method which was powder synthesis technique to prepare their superconductors ($Tl_2CaBa_2Cu_2O_8$ and $Tl_2Ca_2Ba_2Cu_2O_8$). To prepare their 2122 compound, they used stoichiometric mixture of Tl_2O_3, $CaBa_2CuO_4$ and CuO, and to prepare 2223 compounds they have used are Tl_2O_3, CaO, $CaBa_2CuO_4$ and CaO. Their superconducting samples, have transition temperature T_c more than 100K, took 6 to 23 hours to prepare. They calculated maximum transition temperature 116K for 2122, they achieved 110-118K transition temperature for 2223 single phase superconducting samples. Both superconducting samples (2122 and 2223) have sudden transition and saturated Meissner effect. Using this new powder synthesis technique, the main problem of using powder was its melting, was successively lessen which happen broadly in conventional procedure. This decline was mostly because of the presence of $CaBa_2CuO_4$ in the mixture with the help of which 2122 compound was formed and lower temperature calcination was made possible. In the second two step calcination, the 2122 compound functioned as a precursor for 2223 compound. They took the result that the reaction was because of the inter-calcination of CaO and CuO layers into the present 2122 grains.

S.Mikusu et al [10], introduced their thallium based superconductors $TlBa_2Ca_2Cu_3O_y$. To prepare their samples, they used method called solid state reaction. They performed the X-rays diffraction, SEM technique to studied behavior of their samples. To measure resistivity, they used four prob e method and Quantum design MPMs device to calculate the critical temperature Tc. The MPMs was used to calculate the hysteresis loop of DC-magnetization for the field up to7 Tesla at the temperature of 110K. They take into account that the change in critical temperature (T_c) values happens because of small variation in the starting material of the system $TlBa_2Ca_2Cu_3O_y$. From magnetization, they measured the current density J_c and B_{irr}. By comparison measuring data with Hg-1223, they got result that B_{irr} value for Tl-1223 having T_c 130K have higher value than that of Hg-1223 low T_c samples. However, Y-123 has high value of B_{irr} at 77K then obtained valued of Tl-1223 samples. From Their result they suggested that pinning center is necessary for application at 77K.

2.2 Reviews on "Dielectric properties of superconductors":

Vogel R et al [11], were working on chalcogenide thin films and observed negative capacitance in chalcogenide glasses for the first time and chalcogenide glasses were considered as relaxation materials.

Wu X et al [12], explained that the negative capacitance can be seen in various electronic devices, such as interface states and metal semiconductor Schottky diodes.

Ershov M et al [13], analyzed that the microscopic mechanisms of the negative values of capacitance are different for different electronic devices and have been attributed to the interacting injection, as GaAs, AlGaAs and QWIPS (quantum well infrared photodetectors).

Ş Çavdar et al [14], reported dielectric properties and ac conductivity of thallium based ceramic samples, $Tl_2Ba_2Ca_2Cu_3O_x$ (2223) and $Tl_2Ba_2Ca_1Cu_2O_x$ (2212), at different temperature (80-300K) and frequency (100-10MHz). They observed negative capacitance in their materials. They explained that the negative values of real dielectric constant can be calculated from the negative capacitance, according to them term negative capacitance means that the decrease in the capacitance of the device from geometrical capacitance to the negative values and this negative capacitance also shows the variations in the current of the device lags behind the voltage just like inductors. They described that at low frequencies, the real dielectric constants indicate strong dispersion at all different temperatures, the real dielectric constant decreases with decreasing frequency and the real dielectric constant increases with the increase in frequency at all different temperatures and remains constant at higher frequencies. They also explained that at the high frequencies, the huge increase in capacitance may be ascribed to blocking of charges at the electrodes.

They described that the imaginary part of dielectric constant ε_i increases with decreasing temperature and frequency. Imaginary dielectric constant shows strong dispersion at small frequencies. But the dielectric dispersion in the real part is stronger than in the imaginary part.

For their samples, they explained that dispersion in dielectric loss was found shifted towards low frequencies with decrease in frequency and temperature. They observed increase in ac conductivity with decreasing temperature and frequency.

M. Mumtaz et al [15], worked on $Cu_{0.5}Tl_{0.5}Ba_2Ca_3(Cu_{4-y}Cd_y)\ O_{12-\delta}$ (y=0,0.25,0.5 and 0.75) and explained their real dielectric constant ε_r', is the portion of the energy stored in the superconducting material, when sample exposed to field. The negative values of ε_r' (real dielectric constant) can be calculated from the negative capacitance (term that shows a decrease in capacitance of a superconducting sample from geometric capacitance without superconducting sample). And this happens due to the growth of positive charges near electrodes. These charges are probably to gathered at the outer layer of the device just because of the flow of the negative charges flow toward the electrodes. As fermi energy levels are high for ceramics, so the passage of electrons from these ceramics to metal surfaces is possible. The negative capacitance can be observed within the samples in the low frequency range. The reason of negative capacitance is different for each material and it is microscopic physical phenomena associated the trapping of charge carriers, contact injection and effect of space charges. They explained that the imaginary part gives attenuation and absorption of energy along the surfaces (grain boundaries, localized charge densities and localized defects). They concluded that dielectric loss increased in all samples after post annealing in oxygen

M. Mumtaz et al [16], synthesized (CuO, CaO_2 and BaO) $_y/Cu_{0.5}Tl_{0.5}Ca_2Cu_3O_{10-\delta}$ (y=0, 5%,10% and 15%) and described that at high frequencies the real dielectric constant rapidly decreased due to reduction of dipolar polarization. They described that the time period 'T' of oscillation of the external applied field is too quick as compare to the time of dipolar polarization. They conclude that as frequency increases, the ac conductivity decreases.

Wagner KW [17], explained the phenomenon of electric dispersion, according to this phenomenon electric medium should be made of good conducting grains and separated by less conducting grain boundaries. So grains have more permittivity than boundaries. They stated that at small frequencies, these boundaries were extra effective, due to which electric charges were hopping and result in higher dielectric constant. They also observed decrease in imaginary dielectric with increasing frequency which is due to decline in polarization as they (dipoles) do not have capacity to track the externally applied field at large frequencies.

Nawazish Ali Khan et al [18], studied frequency dependent dielectric properties 0f $Cu_{0.5}Tl_{0.5}Ba_2Ca_2Cu_{3-y}Zn_yO_{10-\delta}$ (y=0, 1, 1.5, 2, 2.5) and showed that at low frequency, negative values of dielectric constant are due to the reduction of the capacitance of superconducting samples from the capacitance (geometric) without superconducting samples. So positive charges start neighboring the electrodes due to these movements mobile charges were

displaced from their mean positions and they generated dipolar capacitance. The positive space charges were at the outer surface of the device and negative charges were flowing toward the electrodes from material. The fermi level of metals is lower than ceramics, that's why electrons can flow from ceramic to metals.

Ghazala Y [19], synthesized $Bi_{1.6}Pb_{0.4}Sr_2Ca_{2-x}Mg_xCu_3O_{10+\delta}$ ($0 \leq x \leq 0.5$) to analyzed dielectric properties, they explained the real dielectric constant at high frequencies and it approached at almost same values for samples. She explained that the time constant of dipolar polarization is greater than the time constant of applied field and material have had minimum polarization and she explained imaginary part of dielectric constant as the energy absorption and attenuation across the interfaces. These interfaces can be localized defects, localized charge densities or grain boundaries.

Salma M et al [20], worked on $Bi_{2-x}(CuPb)_xSr_2Ca_2Cu_3O_{10+\delta}$ (x=0, 0.4, 0.5) samples to study effect of dielectric permittivity and conductivity. In real dielectric constant, they observed sudden decrease with frequency, they also described that the imaginary part of dielectric constant has greatest values at the start, as we keep increasing frequency than imaginary dielectric constant decreases immediately because the active component or ohmic component of current increases more suddenly than its reactive component or capacitive component.

References:

[1]. Sheng Z Z and Hermann A. M.: Nature (1988).

[2].L. Perez. Arrieta and M. Aguilar-Frutis Revista Mexicana Defisica, 54 (6)(2008) 446–450.

[3].N. Hassan and N. A. Khan: Materials Chemistry and Physics, 112 (2), (2008) 412-416.

[4].S. Isber, R. Awad, A. I. Abou-Aly, M. Tabbal and J. M. Kaouar: Superconductor Science and Technology, 18 (3) (2005) 311.

[5].N. A. Khan and M. Shamraiz, Journal of Physics: Conference Series 439 (1),(2013) 012022.

[6].A.Iyo, Y. Aizawa, Y. Tanaka, M. Tokumoto, K. Tokiwa, T. Watanabe and H. Ihara, Physica C: Superconductivity, 357–360, Part 1 (0),(2001) 324-328.

[7].N. A. Khan and M. Arif, Physica C: Superconductivity 488 (0), (2013) 35-38.

[8].Y. Shimakawa, Y. Kubo, T. manako, and H. Igarashi: Physical review B, Vol 40, (1989).

[9].Nae-Lih Wu, Yeong Der Yao, Sern- Nan Lee, S- Yen Wong, and Eli Ruckenstein: physica C ,161(1989) 302.

[10]. S Mikusua, G Watanabea, K Tokiwaa, Y Tanakab, A Iyob, and T Watanabea: Journal of Physics: Conference Series, 150(2009) 052161

[11]. Vogel R and Walsh P.: J. Appl. Phy. Lett.14(1969)216.

[12]. Wu X, Yang E S and Evans H L.: J. Appl. Phys. 68(1990) 2845.

[13]. Ershov M, Liu H C, Li L, Buchanan M, Wasilewski Z. R. and Jonscher A. K.: IEEE Trans. Electron Dev 45 (1998)2196.

[14]. S çavdar, H Koralay, N Tugluoglu and Günen: Superconductor science and technology, 18(2005)1204-1209.

[15]. M. Mumtaz, M Rahim, Nawazish A. Khan, K Nadeem and Khurram Shehzad: Cer. Int. 39(2013) 9591-9598.

[16]. M. Mumtaz, M. Kamran, K. Nadeem, Abdul Jabbar, N. A. Khan, Abida Saleem, S. Tajamul Hussain and M. Kamran: low Tem. Physics, 39(2013)806-813.

[17]. Wagner KW. Zur Theorie der unvollkommenen Dilecktrika. Annalen der physics 345 (1913) 817-855.

[18]. N. A. Khan, M Mumtaz and A.A. Khurrum: J Appl. Phys. 104,(2008) 033916-033916-6.

[19]. Ghazala Y. Hermiz: Int. Jour. Of Innovative research in science, Engineering and Technology,3, (2014)8564-8572.

[20]. Salma M Shaban, Bushra Salman Mahdi, Matii N. M. and Radd M. S. Al Haddad: IJAIEM, 2, (2013)217-221.

CHAPTER # 3

Experimental Techniques

Introduction:

This chapter briefly explains the methods of preparation of thallium based high temperature superconductors, different apparatus and procedures were used to study the properties and characterization of superconducting samples and to measure dielectric measurement of these superconductors.

3.1 Sample preparation:

To prepare samples $Cu_{0.5}Tl_{0.5}Ba_2Ca_2Cu_3O_{10-x}$ and $Cu_{0.5}Tl_{0.5}Ba_2Ca_2Cu_{1.5}M_{1.5}O_{10-x}$ (M=Cd, Zn, Ni) which are based on thallium. We used solid state reaction method which consists of two stages. At first stage we prepared precursor for our samples by mixing and ground $Ba(NO_3)_2$, $Ca(NO_3)_2.4H_2O$, and Cu(CN) in early measured ratios of these compounds using mortar and pestle for one hour then using quartz boat we placed this powder material in heated furnace (860°C) for first 24 hours. After 24 hours, furnace was cooled to room temperature and the precursor was again mixed and grounded thoroughly using quartz mortar pestle. Using alumina boat, we placed our sample in furnace at 860C for more 24 hours. The precursors were chilled to room temperature after heating. Then we added suitable measured amount of Tl_2O_3 in the precursor and grounded further for one another hour in mortar for proper mixing. Using hydraulic press, pellet of this mixed precursor was formed by applying 5 tons/cm^2 of pressure. For sintering, the pellet was wrapped in gold foil and placed in pre heated furnace at 860^{0}C for 10 mints, and then reduced to room temperature for stable form of 1223.

3.2. Characterizations:

There are following techniques for the characterization of the superconducting samples,

- X-Ray Diffraction
- Electrical resistivity measurements
- Susceptibility measurement
- Fourier transform infrared spectroscopy
- Dielectric measurements and ac conductivity

3.2.1. X-Ray Diffraction:

X-ray diffraction is a technique to identify the phase of crystal structure of the materials [1] and also provide information about the unit cell. X-rays are very energetic electromagnetic radiations with small wavelengths (order of 0.01 to 10 nm). For diffraction, the size of atoms of the object should be comparable to wavelength of X-rays. Basically it is not possible to make a well diffraction grating which can satisfy the conditions of X-rays diffraction. So the spacing between regularly arranged lattice atoms of crystal is almost equals to the order of wavelength of X-rays. As the crystal has natural grating which can be used for diffraction.

3.2.1.1 Energy of X-ray Photon:

The energy of X-ray photon is,

$$E = h\vartheta \quad \text{..... (3.1)}$$

or $$E = hc/\lambda$$

If $\lambda = 0.0998\text{nm}$, as $hc = 1240\ \text{ev.nm}$

$$E = 12.42\ \text{Kev}$$

X-rays should be in range of 10KeV to 50KeV to study the crystalline structure of materials. The X-rays photons with these energies (10KeV to 100KeV) can penetrate below the layer of a crystal and create the roots for many conventional methods for examination of unknown 3D structures.

3.2.1.2 Advantages and Disadvantages of X-rays:

There are some advantage and disadvantage of x ray diffraction, which are

- X-ray diffraction is widely used technique.
- X-ray diffraction is economical and appropriate method.
- X-rays are not very absorbable by air and sample do not needs to place in vacuum.
- X-ray diffraction is fast, easy and non-destructive method.
- X-rays can be detected by a photographic film.
- X-rays cannot strongly interact with the lighter atoms.
- X-rays cannot specify the existence of different isotopes of the similar element.

3.2.1.3 Bragg's Law:

William Henry Bragg and his son William Lawrence Bragg, who proposed the X-rays diffraction for the first time [2]. They found that crystalline materials, at some wavelength

and initial angle, produced strong reflection. The idea of Bragg's law can be applied on both electron and neutron diffraction but their wavelength should be comparable to inner distance of atoms. As X-rays are very energetic electromagnetic waves with very small wavelength but it is possible to study diffraction of X-rays by crystals. In a crystal, the atoms are regularly arranged in planes and distance between these planes is equal to the wavelength of X-rays. Therefore, a crystal behaves like a 3D grating.

Let there are two incident monochromatic X-rays 'a' and 'b' of wavelength 'λ' are reflected from the two consecutive planes separated by distance 'd' known as inter-planar spacing. Let the incident beam makes an angle θ (glancing angle) with the crystal plane.

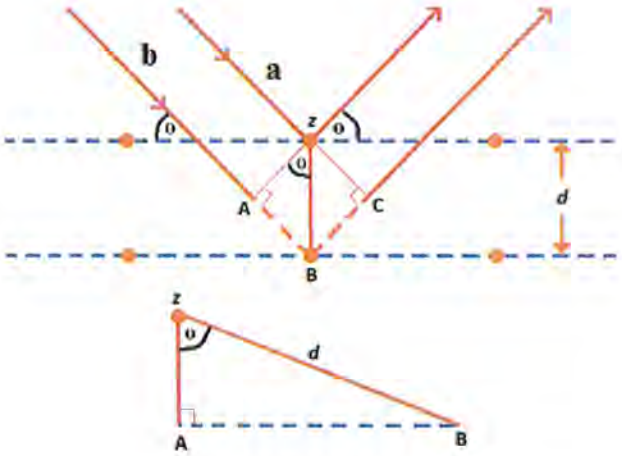

Fig. 3.1: X-rays diffraction from crystal planes

For path difference 'd' between these two X-ray beams, so we draw perpendiculars from Z to A and C. Hence

$$\text{Path difference} = AB + BC$$

From fig,

$$AB = d \sin\theta \quad \text{..... (3.2)}$$

And Similarly,

$$BC = d \sin\theta$$

So,

$$\text{Path difference} = d \sin\theta + d \sin\theta$$

$$\text{Path difference} = 2d\sin\theta$$

These reflected beams interfere constructively interference and we will see a bright spot on the screen (photographic plate). These rays remain in phases since their path difference is equal to the integer multiple of wavelength λ. Path difference is equal to 2d sinθ and condition for constructive interference [3].

$$2d\sin\theta = n\lambda \ldots\ldots\ldots\ldots\ldots \textbf{(3.3)}$$

This is Bragg's law. Here n is positive integer (n=1, 2, 3 ...) and λ wavelength of incident X-rays. If the wavelength of X-rays is known, then we can easily find the inter-planar spacing 'd'. Using Bragg's law, the study of crystal structure has formed the basis for X-ray crystallography.

3.2.1.4 X-Ray Diffraction Techniques:

- X-ray diffraction is used to study the structure of a sample that either the sample has amorphous or crystalline structure. XRD graph displays their structure. If material of the sample is crystal, then graph will show various and sharp intensity peaks which reveals that material has periodic structure but in amorphous structure, the graph of X-ray diffraction shows only one or two sharp intensity peaks [4].
- In multicrystalline or polycrystalline materials, we can calculate grain size by using the full width half maxima (FWHM) rule. The formula is,

$$S = \frac{0.9\lambda}{A\cos\theta_B}$$

S= grain size, λ = wavelength of X ray, θ_B = Bragg's angle, A = full width half maximum

The full width at half maximum is

$$A = 1/2\ (2\theta_1 - 2\theta_2)$$

- The density of the unit cell is given by the formula

$$\rho = \frac{\Sigma A / N_A}{V}$$

Where

ΣA = sum of atomic weights of all atoms N_A = Avogadro's number V = Volume of unit cell

3.2.1.5 X-ray diffractometer:

In figure 3.2. a diffractometer is shown. A sample is supported by a smooth plate in such a way that it could rotate about an axis which is in direction perpendicular to the surface of the paper. Monochromatic X-rays are formed in x-ray tube and by passing the rays from a slit. The beam fall upon the specimen and diffraction takes place. The intensities of beams, which are diffracted, are noticed with a counter. The source of x-rays, specimen and counter all are in one plane. The counter can rotate about its axis.

The angular location of the counter is measured in term of 2θ. The counter and the specimen are arranged in such a way that if the specimen is rotated through an angle, counter is rotated through 2θ, because of this the angle of incidence and the reflection angle are remained

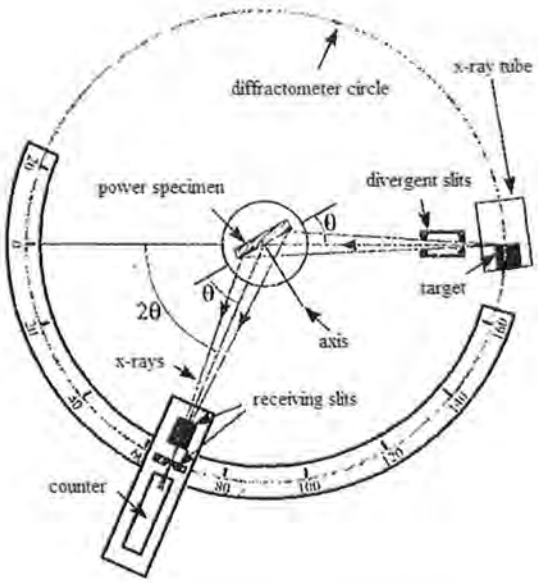

Fig. 3.2: X-rays diffractometer

constant. As the angular velocity of the counter remains constant the intensities of diffracted rays is recorded as a function of 2θ. The data that is obtained from the diffractometer is examined for finding the crystal arrangement of the specimen. Computer software 'chekcell' is used for finding the matrix parameters and the identification of crystal arrangement.

3.2.2 Electrical Resistivity:

Temperature 'T' and the average time 'τ' are two main reasons for electrical resistivity.

3.2.2.1 Dependence on average time 'τ':

When external electric field is applied to the sample, the electrons of the atoms get accelerated and they started colliding with the atoms. Thus the resistance is offered by the atoms to the flow of electrons. This resistance is because of collision and resistivity is given by,

$$\rho = \frac{m}{n\tau e^2} \quad \text{..... (3.4)}$$

Where 'ρ' is resistivity, m is mass of electron, 'τ' is average time between two collisions, $\frac{1}{\tau}$ is the probability of electron collision (scattering) per unit time and 'n' is the number density. As we know that every crystal has imperfections. So when electrons flow, they can face collision with lattice phonons. Therefore, the total probability of electron to happen a collision (scattering) is equal to scattering of electron from phonons $\frac{1}{\tau_{ph}}$ and lattice imperfections $\frac{1}{\tau_i}$. So total probability is,

$$\frac{1}{\tau} = \frac{1}{\tau_{ph}} + \frac{1}{\tau_i} \quad \text{..... (3.5)}$$

So resistivity is,

$$\rho = \rho_{ph} + \rho_i \quad \text{..... (3.6)}$$

Where 'ρ_{ph}' is the ideal resistivity and it is temperature dependent while 'ρ_i' is the residual resistivity does not dependent on temperature [5] .

3.2.2.2 Dependence on Temperature:

When temperature of a superconducting sample increases, the collision of electrons with the atoms also increases so resistance increases and when sample is cooled (temperature is lowered) then collision with atoms decreases so resistance decreases. And we know that the temperature dependent resistivity 'ρ_{ph}' is due to phonons. So at low temperature, the dependence of resistivity on temperature is of the order of T^5 and it is confirmed for alkali

metals. In simple metals, at high temperatures, the dependence of resistivity on temperature is the mean square amplitude of phonons.

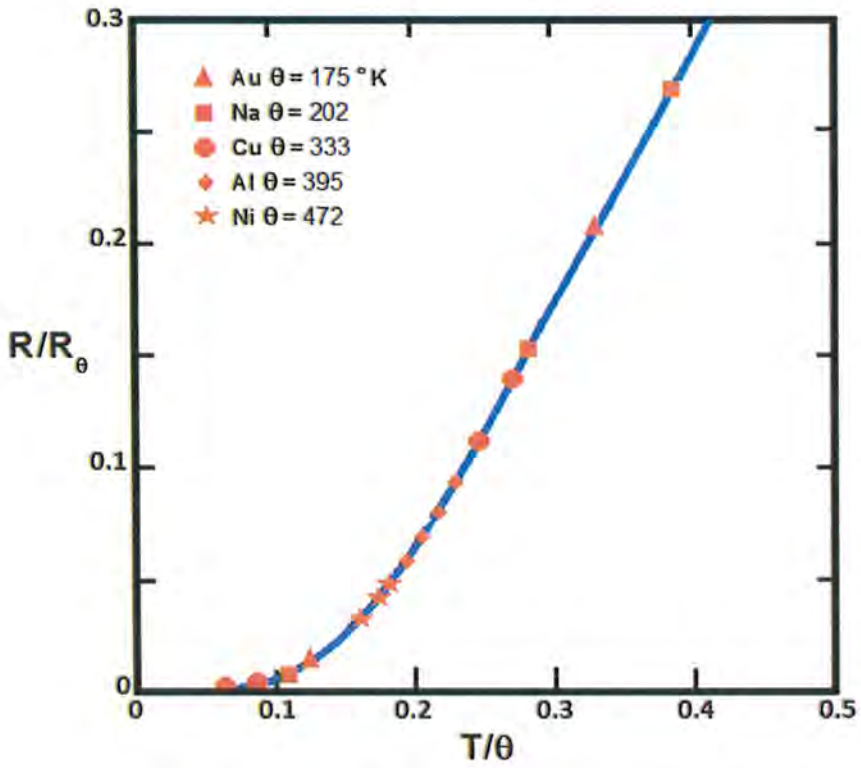

Fig. 3.3: The phonon contribution to the resistivity in normal metals.

3.2.2.3 Electrical resistivity measurements:

Using DC electrical resistivity, we can measure critical temperature 'T_c' of superconducting sample and it helps us to analysed their properties in superconducting and normal states. DC-electrical resistivity is measured by four probe method which is founded on **Ohm's Law,** which is

$$V = IR$$

Where 'I' is the current applied, 'V' is the voltage and 'R' is the resistance of the conductor.

Experimentally, the resistance is proportional to the length 'L' of conductor and inversely proportional to the area of cross-section 'A'. So,

$$R \propto L$$

and

$$R \propto \frac{1}{A}$$

Or,

$$R \propto \frac{L}{A}$$

Can be written as,

$$R = \rho \frac{L}{A}$$

Where constant 'ρ' is called resistivity and it is the function of temperature.

$$R(T) = \rho(T)\frac{L}{A}$$

$$\rho(T) = R(T)\frac{A}{L} \quad \text{..... (3.7)}$$

But from the Ohm's law

$$R(T) = \frac{V}{I}$$

$$\rho(T) = \frac{V}{I}\frac{A}{L}$$

$$\rho(T) = \frac{VA}{IL} \quad \text{..... (3.8)}$$

If area 'A' is in m^2, length 'L' in m, current 'A' in amperes and voltage 'V' in volts, then the unit of the resistivity becomes Ω-m'.

3.2.2.4 Methods of Resistivity Measurement:

The aspect which is affecting the appropriateness of techniques including resistance and the structure (shape) of a sample i.e. whether in the form of powder, a single crystal film or small crystalline [6].

Our superconducting samples are in the form pellets (small crystals) which are copper thallium based. The resistivity can be calculated using equation (3.8) where 'I' is the constant current and 'V' is the voltage drop across the superconducting sample.

3.2.2.5 Four Probe Method for resistivity:

This system is extensively used for the calculations of resistivity of semiconductors, metals, and superconductors. Fig. 3.4 displays the experimental setup for four-probe method.

In this technique, there are four contacts which are connected to surface of the superconducting sample and these the connections are made by silver paste. Two outer leads are for the current 'I' through the superconducting sample while the inner two are for voltage drop across the superconducting sample. This voltage drop can be observed due to the resistance to the flow of current across the sample.

Here in this method, we can measure the voltage drop across the probes '1' and '2', the current 'I' passing through the contacts '3' and '4' the separation 'D' between probes '1' and '2' and the cross-sectional area 'A' of the sample.

After measuring these parameters for superconducting samples, relation for resistivity is,

$$\rho(T) = V(T)A/ID$$

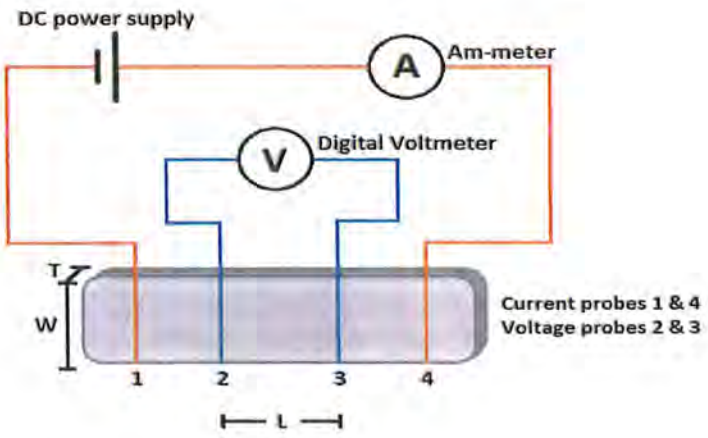

Fig. 3.4: Schematic of four-point probe

Where voltage drop is temperature dependent. There are some steps which are,

1. The source of constant current was constructed by connecting the MW2122A regulated DC power supply in series with resistance.
2. A micro-ammeter was connected in series, which can calculate current up to $1000\mu A$ with an accuracy of 1 μA
3. The P-2000/E KEITHLEY MULTIMETER was used to calculate voltage drops across the superconducting samples at in different temperatures.
4. Temperature of the sample was calculated by thermocouple in mV.
5. A simple cryostat consisting of liquid nitrogen Dewar and a brass pipe fitted with a sample mount at one end and connecting wires at the other was used as sample holder.

3.2.3 Ac magneto susceptibility technique:

Susceptibility is originated from Latin word 'susceptibilis' which means receptive; basically magnetic susceptibility is measure of magnetic property of a sample. So susceptibility is the word used for the response of any sample to the externally applied magnetic field. Every conducting sample has magnetic behaviour, whether a sample is attractive or repulsive toward magnetic field lines. Some materials show high magnetic response i.e. ferromagnetic, some are materials have low magnetic response i.e. paramagnetic, and some are those which have magnetic response only in external magnetic field.

Magnetism has microscopic behaviour. As we know that moving electron (charges) produces magnetic field, as electrons of atoms rotates around the nucleus and produces very small current and this current generates a magnetic moment. As electrons keeps on spinning around its axis and produces spin magnetic moment. These magnetic moments are measured in the unit of Bohr magneton μ_B. When a conducting material have two alignments (in specific direction) i.e. spin magnetic moments and orbital magnetic moments then magnetic field arises and material behaves like a magnet. However, usually material do not display their magnetic behaviour unless they are placed in the external magnetic field, because of random alignments of magnetic dipoles in material, the net magnetic moment is zero.

The magnetic induction 'B' is a process by which material becomes magnetized in external magnetic field, while H is magnetic field strength and both can be related as,

$$B = \mu_{\circ} H \quad \ldots\ldots\ldots\ldots\ldots\ldots \textbf{(3.9)}$$

Where $\mu_\circ$ is permeability of free space. When a substance is in an external magnetic field then there will be magnetization in the substance and the magnetic dipole of the substance align in the direction of applied field so,

$$B = \mu_\circ H + \mu_\circ M \quad \ldots\ldots\ldots\ldots\ldots\ldots (3.10)$$

Let 'M' is the magnetization of the substance, dividing by H above equation,

$$\frac{B}{H} = \mu_\circ\left(1 + \frac{M}{H}\right)$$

In medium we have,

$$B = \mu H$$

Or,

$$\frac{B}{H} = \mu$$

Here μ represent the permeability of the medium.

Let χ be the susceptibility of the substance, which is amount of magnetization [7]

$$\frac{M}{H} = \chi$$

So above equation becomes

$$\mu = \mu_\circ(1 + \chi)$$

$$\frac{\mu}{\mu_\circ} = 1 + \chi \quad \ldots\ldots\ldots\ldots\ldots\ldots (3.11)$$

Let $\mu_r = \frac{\mu}{\mu_\circ}$ is the relative permeability of the substance.

Or equation 3.10 can be written as,

$$\chi = \mu_r - 1$$

And value of susceptibility determines the magnetic nature of material (substance). If $\chi > 1$, the material is ferromagnetic and $\chi < 1$ for diamagnetic material.

Superconductors are perfect diamagnetic materials having $\chi < 1$, so χ Become complex and can be written as,

$$\chi = \chi' + i\chi''$$

The imaginary part arises due to the changing magnetic field [8], its shows hysteresis loss and real part shows the shielding effect of the superconducting samples.

For ac susceptibility χ can written as,

$$\chi = \frac{dM}{dH_{AC}} \quad \ldots\ldots\ldots\ldots\ldots\ldots \textbf{(3.12)}$$

The real part of the complex susceptibility is out of phase by 90° with imaginary part but in phase with the magnetic field. As phase diagram,

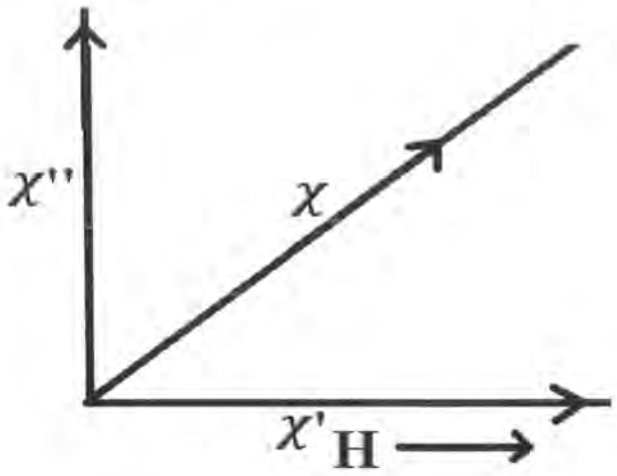

FIGURE 3.5: PHASE DIAGRAM

High temperature superconductors (multi-crystalline or polycrystalline) have complex crystal structure. In polycrystalline the susceptibility transition takes place in two-step, firstly, the transition happens in grains and then the transition happens in the decoupling of the grains.

The value of critical magnetic field, require for interior transition is larger than decoupling of these grains. Before entering the grains, external field decouples these grains. When $T < T_C$ (Below T_C) the current cannot pass into the samples because of flux lines and bulk of sample reflecting it. Anyway, when temperature increases, the current start piercing

into material. And for $T < T_C$, current near the boundary of the sample developed because of induce current that was generated by externally changing magnetic field. As we increase magnetic field, the imaginary part of the magnetic susceptibility has broadened peaks and at high temperature which is greater than peak temperature, the grains are decouple [9].

3.2.3.1 AC Magnetic Susceptometer:

The magnetic susceptibility of superconductors can be calculated by using ac magnetic susceptometer.AC susceptrometer has four main parts,

- Coil assembly
- Sample holder
- Cryostat
- Electronic circuit

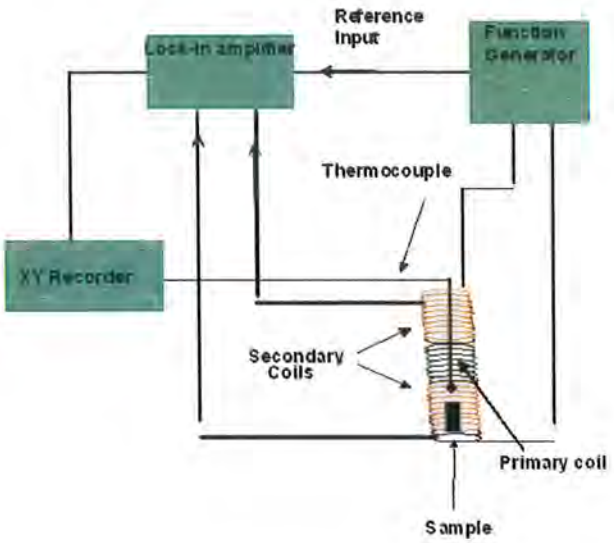

Figure 3.6: Experimental arrangement of Ac magneto susceptibility.

This susceptometer works on the mutual induction and it is set in the coils. There are two coils in susceptrometer, primary and secondary coil. The primary coil produces ac field and the secondary coil is more parted by two oppositely coils which can pick diamagnetic signal. There is no flux in the secondary coils because opposite direction of both loops. There are some other parts of susceptometer like plotter, locking in amplifier and frequency generator.

The purpose of lock in amplifier is to amplify the signal, primary coils produces amplified signal which comes from secondary coils. We can adjust frequency of primary coil using the

frequency generator. The graph plotter is used to plot the graph. For plotting graph, pellet is connected to thermocouple and placed in secondary coil, by cooling below critical temperature we can take measurements at different temperature.

In calculation of Ac susceptibility of superconducting sample, 1volt ac signal with of 270hz frequency is applied to the primary coils which induce electromotive force in the secondary coils, which displays that the magneto susceptometer works as bridge network. The lock in amplifier is used for the display of signal which was amplified from the secondary coil.

3.2.4 Fourier Transform Infrared Spectroscopy:

In solid, atoms of materials vibrate with frequency about their mean positions. These vibrations depend on the mass of atom, bond angle and bond length. Even at 0K temperature, their atoms vibrate. Lattice vibrations are very necessary to explain the physical properties of the materials. For scharacterization, we need to determine which type of vibrational modes are present in a given material.

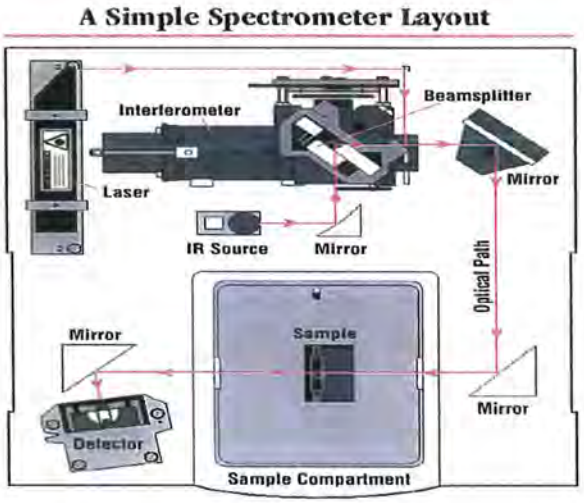

Figure 3.7: The diagram of FTIR instrument

To study these modes, we use a technique known as Fourier transform infrared radiation (FTIR) spectrometer or FTIR spectroscopy.

3.2.4.1 Components of FTIR:

These are some components of FTIR, which are

- Michelson Interferometer

- Light source or laser
- Sample
- Detector
- Computer

- Michelson interferometer:

Michelson interferometer is important part of FTIR spectrometer. Michelson Interferometer contains,

- A moving mirror
- A fix mirror
- Detector
- A beam splitter

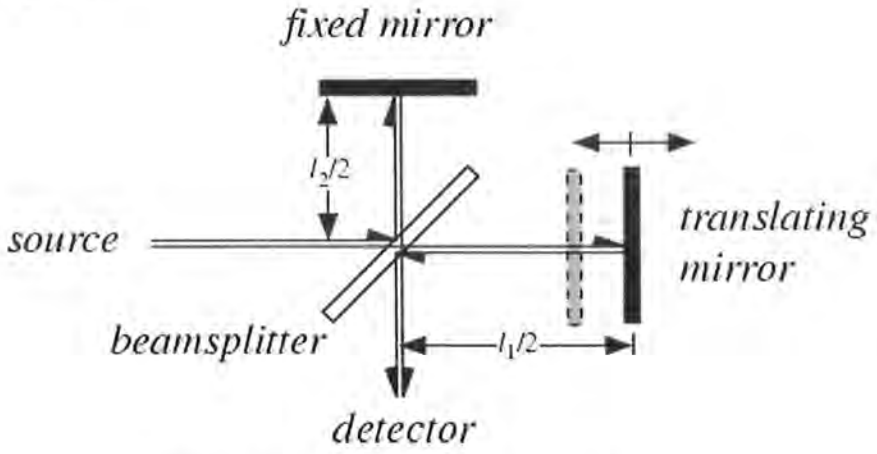

Figure 3.8: Michelson interferometer.

Both mirrors (fixed and moving) are plane and perpendicular plan. In these mirrors, one mirror is stationary and other can move perpendicular to the first one. Another part of FTIR apparatus is the beam splitter is a device, which splits the light of source into two parts, some of the light reflects and some transmit. The reflected beam moves towards the fixed mirror after striking and then reflects.

The information about frequency that how much frequency has been absorbed by the material (sample) and save in interferogram[10]. The interferogram can convert the intensity versus frequency IR spectrum by Fourier transformation [11].

- **The source:**

Beam Infrared rays is discharged from a shining source. This beam (rays) passes through the gap in order to control the amount of energy entering the sample and ultimately reaching the detector.

3.2.4.2 Procedure:

In order to study the modes of vibrations in superconducting samples, the FTIR spectrum has the following steps,

- We used OMNIC software to analyse and studied the spectrum of our samples.
- Firstly, we placed KBr pallet placed in the path of the beam as a background and 300 scans were taken, by setting range of 400-700 cm^{-1}.
- We added approximately 5 mg of superconductor in 50 mg KBr compound, mixed them properly and made the pallet. Again we took 300 scans of the mixed sample spectrum and range was already set at 400-700 cm^{-1}.
- As we used KBr as background and after subtracting the background spectrum, the computer only displayed spectrum of our sample.

3.2.5 Dielectric measurements and ac conductivity:

To calculate real and imaginary dielectric constants (ε' and ε"), dielectric lose (tan δ) and ac conductivity, the conductance (G) and capacitance (C) were measured directly in frequency and temperature ranges of 20Hz-1MHz and 80K- 290K with an LCR meter.

3.2.5.1 Procedure:

Before measuring the values from LCR meter, the calibrations were made with the aid of typical inductor and capacitor to clarify any effect of external circuit.

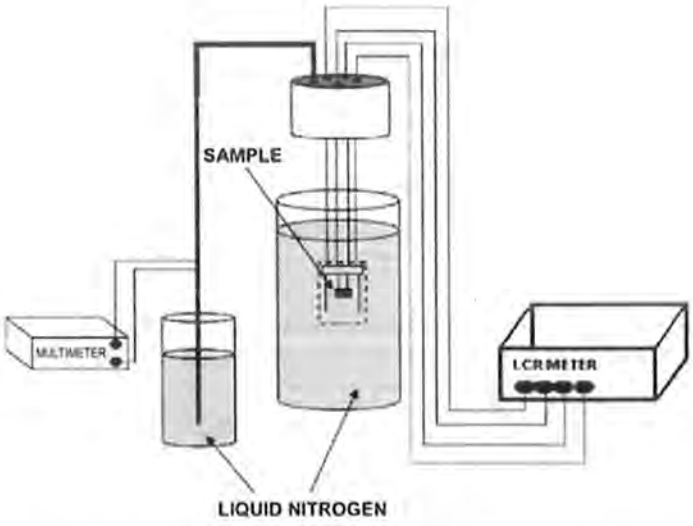

Figure 3.9: Experimental setup for dielectric properties.

For these calculations, the parallel mode was used. A two probe method was used for the calculations of samples pellets. The silver paste was applied on the both sides of sample, thin conducting wires were fixed on silver electrode sides and sample was dried at room temperature. To calculate capacitance and conductance as a function of frequency, the sample pellet was connected to electric connection including LCR meter. Liquid nitrogen was used to decrease temperature of superconducting samples. By calculating capacitance (C) and conductance (G) at different values of temperature and frequency, the dielectric constant (ε_r', ε''_i) , dielectric loss ($\tan\delta$) and ac conductivity (σ_{ac}) were determined using equation [12],

$$\varepsilon_r' = Cd/A\varepsilon_O$$

$$\varepsilon_i'' = Gd/A\varepsilon_0\omega$$

$$\tan\delta=\varepsilon_i''/\varepsilon_r'$$

$$\sigma_{ac}=2\pi f\varepsilon_0\varepsilon'_r\tan\delta$$

where A is area of electrode, d is thickness, C is capacitance, G is conductance, $\omega(2\pi f)$ is angular frequency, f is frequency of applied field, ε_0 is permittivity of free space.

References:

[1]. J. S. Blakemore, Solid State Physics, Cambridge University Press, (1985).

[2]. Bragg W.H; Bragg W.L, Proc. R.: Soc. Lond,88(1913)428-438.

[3]. B. E. Warren, X-ray Diffraction.Dover Publications, (1969).

[4]. J. S. Blakemore, Solid State Physics, Cambridge University Press, (1985).

[5]. A Simplified Approach to the Solid State Physics, M.N Rudden, A.Inst. P.J. Wilson, (1971)

[6]. K. Lark-Horouitz and Vivian A.Johnson,Academic Press, New York and London (1959)401-402.

[7]. S. N. Putilin, E.V.Antipov,O.Chrnaissem and M.Marezio,:Nature 362(1993)226-228.

[8]. A.G. Mamalis and D.E.Manolakos, "Technomic Publishing Company,(2000).

[9]. Martin Nikolo: Am. J. Physics,63 (1994).

[10]. J. R. Ferraro and L. J. Basile, Academic Press, 4(1982)345-392.

[11]. F. A. Settle, Handbook of instrumental techniques for analytical chemistry. (Prentice Hall PTR, (1997).

[12]. S çavdar, H Koralay, N Tugluoglu and Güne: Superconductor science and technology, 18(2005)1204-1209.

Chapter # 4

Results and Discussion

4.1 Introduction:

The substitution of metallic impurities at the CuO_2 planar sites is essential for the studies of intrinsic mechanism of high T_c superconductivity in oxides [1-8]. In this connection the substitution of magnetic (such as Ni) and non-magnetic impurities (such as Zn and Cd) in the neighborhood of cooper atom play a very vital role [9-18]. Since the Zn and Cd atoms in their ground state has filled $3d^{10}$ and $4d^{10}$ their substitution at the copper would not contribute any magnetic moment but, the doping of Ni would contribute its magnetic moment in the CuO_2 planes. We have synthesized $Cu_{0.5}Tl_{0.5}Ba_2Ca_2Cu_{3-x}M_xO_{10-\delta}$ (M = Cd, Zn, Ni; x=0, 1.5) superconductors and studied their dielectric properties in the low frequency regimes 30Hz-1000Hz. The main objective of doping of M = Cd, Zn, Ni elements with different masses than Cu in $Cu_{0.5}Tl_{0.5}Ba_2Ca_2Cu_{3-x}M_xO_{10-\delta}$ samples was to look into any possible role of electron phonon interaction in the mechanism of high temperature superconductivity in the compound. The solid state medium of $Cu_{0.5}Tl_{0.5}Ba_2Ca_2Cu_{3-x}M_xO_{10-\delta}$ (M = Cd, Zn, Ni; x=0, 1.5) containing free carriers in the CuO_2 planes is expected to get polarized when subjected to external electric field of frequency. Two possible mechanisms of polarization including interfacial and dipolar polarization are possible in the frequency regimes under studies (i.e 40-3000Hz).

The dielectric constant determines the nature of superconducting material i.e. what are the binding forces to which the mobile carriers are tied to between the conducting CuO_2/MnO_2 (M=Cd, Ni, Zn) planes, their interfaces and $Cu_{0.5}Tl_{0.5}Ba_2O_{4-\delta}$ charge reservoir layer. In other words, dielectric measurements would help in determining the coupling strength of their interfaces (i.e CaO planes) and the charges in the charge reservoir layer. The CuO_2/MnO_2 (M=Cd, Ni, Zn) planes coupled with the interfaces of CaO strongly will be marginally polarized imparting lower values to the dielectric constant and vice-a-versa.
Depending on the frequency of applied electric field, a material gets polarized by employing one of the four mechanisms of polarization [19-23] including:
(1) Electronic polarization (α_e) are usually observed at very high frequency of the order of $\sim 10^{15}$Hz (i.e. in ultraviolet optical range)

(2) Atomic and ionic polarization (α_a) are observed in the infrared frequency range (i.e. from 10^{10} to 10^{13} Hz).

(3) The dipolar or oriental polarization observed is (α_o) are observed in the sub-infrared frequency range (10^3 to 10^6 Hz).

(4) Interfacial polarization (α_i) are usually sensitive in the low frequency range (i.e 10^2 Hz) and can extend to a frequency of few kilohertz which mainly contributes to the dielectric properties of the materials in our case.

All of aforementioned mechanisms of polarization involve a short-range motion of charges from their equilibrium position contributing to the polarization of the material [24]. In the dielectric measurements of materials, the dipolar and interfacial polarization play a vital role. The dielectric measurements of $Tl_2Ba_2Ca_2Cu_3O_x$, $Tl_2Ba_2CaCu_2O_x$ [25] $Bi_2Ba_2Nd_{1.6}Ce_{0.4}Cu_2O_{10+\delta}$ [26] and $Bi_{1.84}Pb_{0.34}Sr_{1.9}Ca_{2.03}Cu_{3.06}In_xO_y$ [27] oxide high temperature superconductors have been reported in the frequency range of 10KHz to few MHz and the material exposed to such high frequency range might turn into its normal state. It is therefore essential to characterize such material in the low frequency range in order to have better insight to the essential intrinsic characteristics of the superconducting compound. In the current studies we have used a frequency LCR meter most suitable of the characterization of superconducting compounds. We have studied the dielectric measurements of $Cu_{0.5}Tl_{0.5}Ba_2Ca_2Cu_{3-x}M_xO_{10-\delta}$ (M = Cd, Zn, Ni; x=0, 1.5) superconducting samples in the frequency range of 30Hz to 3000Hz from room temperature (290K) down to 80K.

4.2 Experimental:

The $Cu_{0.5}Tl_{0.5}Ba_2Ca_2Cu_3O_{10-d}$ and $Cu_{0.5}Tl_{0.5}Ba_2Ca_2Cu_{1.5}Y_{1.5}O_{10-d}$ samples (Y=Cd, Zn, Ni) superconductor samples were synthesized by two-step solid-state reaction method. At the first step we have prepared $Cu_{0.5}Ba_2Ca_2Cu_3O_{10-d}$ and $Cu_{0.5}Ba_2Ca_2Cu_{1.5}Y_{1.5}O_{10-d}$ samples (Y = Cd, Zn, Ni) precursor material, by thoroughly mixing the $Ba(NO_3)_2$, $Ca(NO_3)_24H_2O$ and $Cu_2(CN)_2+H_2O$, and then with the $Cd(NO_3)4H_2O$, ZnO, $Ni(NO_3)6H_2O$, compounds in appropriate ratios in a quartz mortar and pestle. The mixed material was then twice fired at 860◦C in a quartz boat for 24 hours, followed by furnace cooling to room temperature. At the second stage, the fired precursor material was again ground for about an hour and mixed with calculated amount of Tl_2O_3 to give $Cu_{0.5}Tl_{0.5}Ba_2Ca_2Cu_3O_{10-d}$ and $Cu_{0.5}Tl_{0.5}Ba_2Ca_2Cu_{1.5}Y_{1.5}O_{10-d}$ samples (Y = Cd, Zn, Ni) as final reactants compositions. Thallium mixed material was then pelletized under 3.8 tons/cm^2 of pressure and the pellets

were wrapped in a thin gold foil. These samples were heat treated for 10 minutes in a preheated furnace at 860°C followed by quenching to room temperature suddenly. This was done because thallium oxide is volatile in nature and it melts at 717°C and vaporizes when heated at higher temperature to avoid this we use gold foil to retain thallium. These samples were characterized by resistivity measurements using the four-probe method and AC-susceptibility measurements using the mutual inductance method. The structure of the material was determined by the X-ray diffraction scan, Bruker DX 8 Focus using a CuKα source of wavelength 1.54056 Å, and the cell parameters were determined by a cell refinement computer program. The Fourier Transform Infrared (FTIR) absorption measurements were carried out using a NICOLET 5700 Fourier Transform Infrared spectrometer. Fourier Transform Infrared (FTIR) spectroscopy was carried out using KBr as a background material with 400-700cm^{-1} wave number ranges. Frequency dependent dielectric measurements of $Cu_{0.5}Tl_{0.5}Ba_2Ca_2Cu_{3-x}M_xO_{10-\delta}$ (M = Cd, Zn, Ni; x=0, 1.5) samples were taken on Wayne Kerr 4275 LCR Meter of frequency range 20-500KHz, however, we have used this LCR meter in the frequency range 30-3100Hz. We have measured the real and imaginary parts of the dielectric constants from room temperature down to 80K.

4.3 Results and Discussions:

The x-ray diffraction scans of $Cu_{0.5}Tl_{0.5}Ba_2Ca_2Cu_{3-x}M_xO_{10-\delta}$ (M = Cd, Zn, Ni; x=0, 1.5) samples are shown in Fig.4.1(a, b). It can be seen from these diffraction scans that most of the planar reflections are fitted to the orthorhombic crystal structure; in the fitting of reflection lines we have followed PMMM space group. The cell parameters calculated have shown that the lengths of a-axis length increases and the b-axis length suppresses with the incorporation of M= Cd, Zn, Ni in final compound. However, suppression in the c-axis length has been observed in all doped samples, Fig.4.2 (a, b)

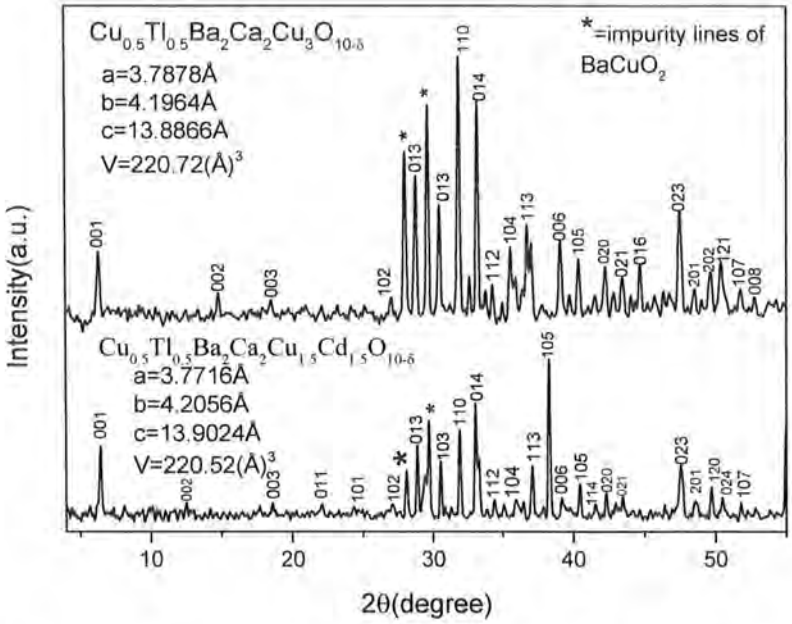

Fig. 4.1(a): X-ray scan of $Cu_{0.5}Tl_{0.5}Ba_2Ca_2Cu_3O_{10-\delta}$ and $Cu_{0.5}Tl_{0.5}Ba_2Ca_2Cu_{1.5}Cd_{1.5}O10_{-\delta}$ samples.

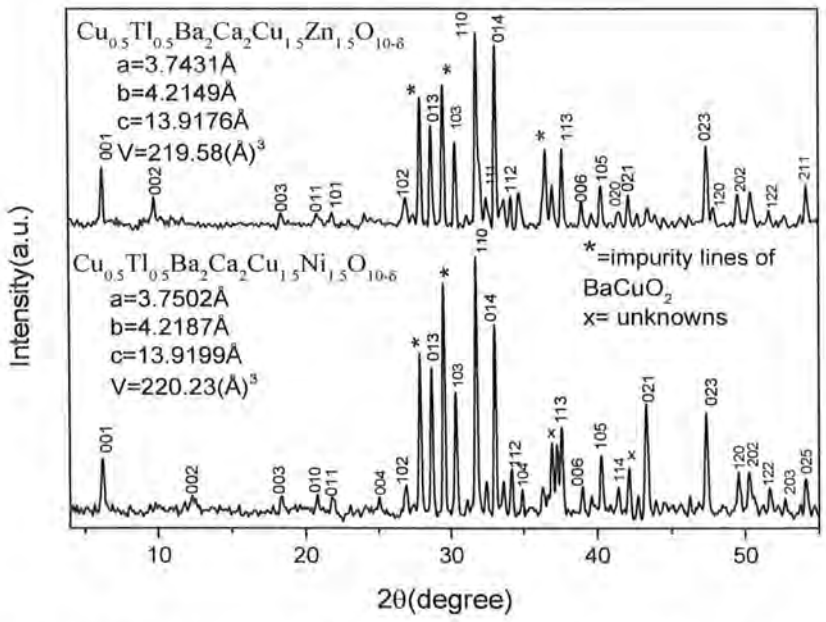

Fig. 4.1(b): X-ray scan of $Cu_{0.5}Tl_{0.5}Ba_2Ca_2Cu_{1.5}M_{1.5}O10_{-\delta}$ (M=Zn) and $Cu_{0.5}Tl_{0.5}Ba_2Ca_2Cu_{1.5}M_{1.5}O10_{-\delta}$ (M=Ni) samples.

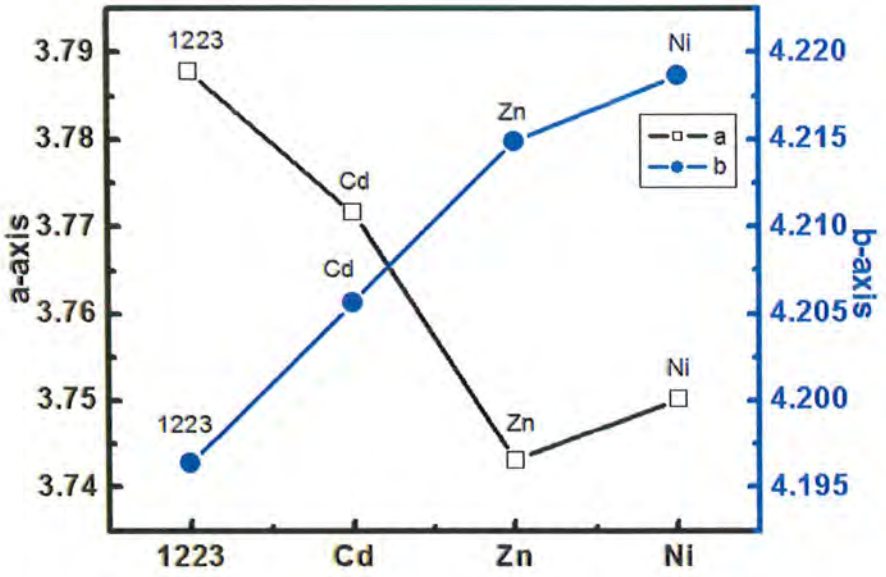

Fig. 4.2(a): The a and b axis comparison of $Cu_{0.5}Tl_{0.5}Ba_2Ca_2Cu_3O_{10-d}$ with M doped $Cu_{0.5}Tl_{0.5}Ba_2Ca_2Cu_{1.5}M_{1.5}O_{10-d}$ (M= Cd, Zn, Ni) samples.

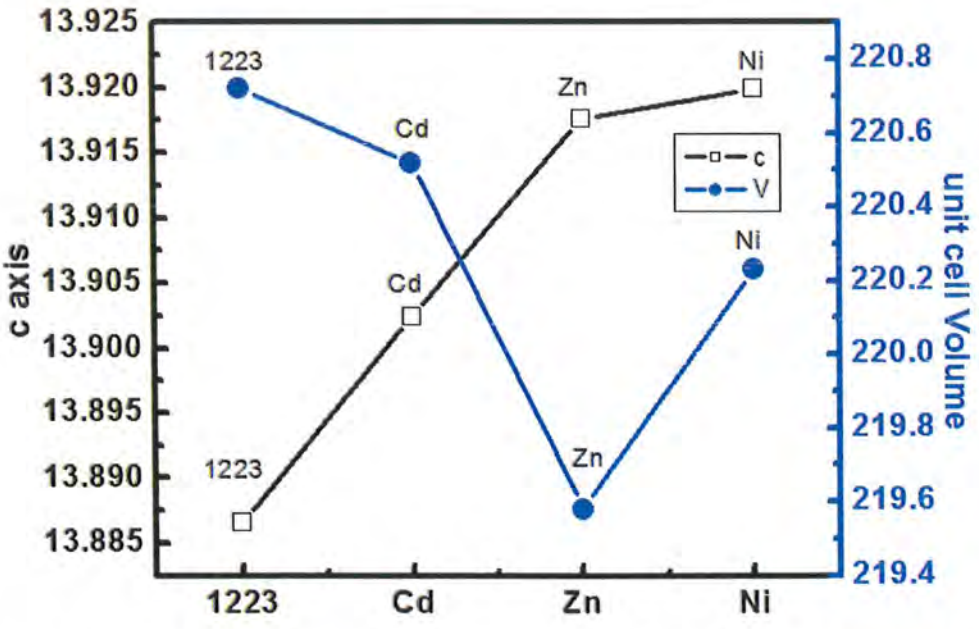

Fig. 4.2(b): The c axis and volume comparison of $Cu_{0.5}Tl_{0.5}Ba_2Ca_2Cu_3O_{10-d}$ with M doped $Cu_{0.5}Tl_{0.5}Ba_2Ca_2Cu_{1.5}M_{1.5}O_{10-d}$ (M= Cd, Zn, Ni) samples.

The resistivity measurements i.e ρ(T), of $Cu_{0.5}Tl_{0.5}Ba_2Ca_2Cu_{3-x}M_xO_{10-\delta}$ (M = Cd, Zn, Ni; x=0, 1.5) sample are shown in Fig.4.3. All these samples have shown metallic variations of resistivity from room temperature down to the onset of superconductivity with onset of superconductivity around 105.6, 101.7, 114, 106.3K and the $T_c(R=0)$ around 98.3, 95.4, 102.3, 102K, respectively, Table 4.1.

Sr.No	Sample	Resistivity			Susceptibility	
		$T_c(R=0)$ K	T_c(onset) K	Resistivity at room temperature (Ω-cm)	Magnitude of diamagnetic	T_c (onset) K
1.	1223	98.3	105.6	0.146	0.069	113.6
2.	Cd	95.4	101.7	0.204	0.079	105
3.	Zn	102.3	114	0.25	0.075	105.2
4.	Ni	102	106.3	0.092	0.068	107.7

Table 4.2. Resistivity and susceptibility of $Cu_{0.5}Tl_{0.5}Ba_2Ca_2Cu_3O_{10-\delta}$ and $Cu_{0.5}Tl_{0.5}Ba_2Ca_2Cu_{1.5}M_{1.5}O_{10-\delta}$ (M=Cd, Zn, Ni)

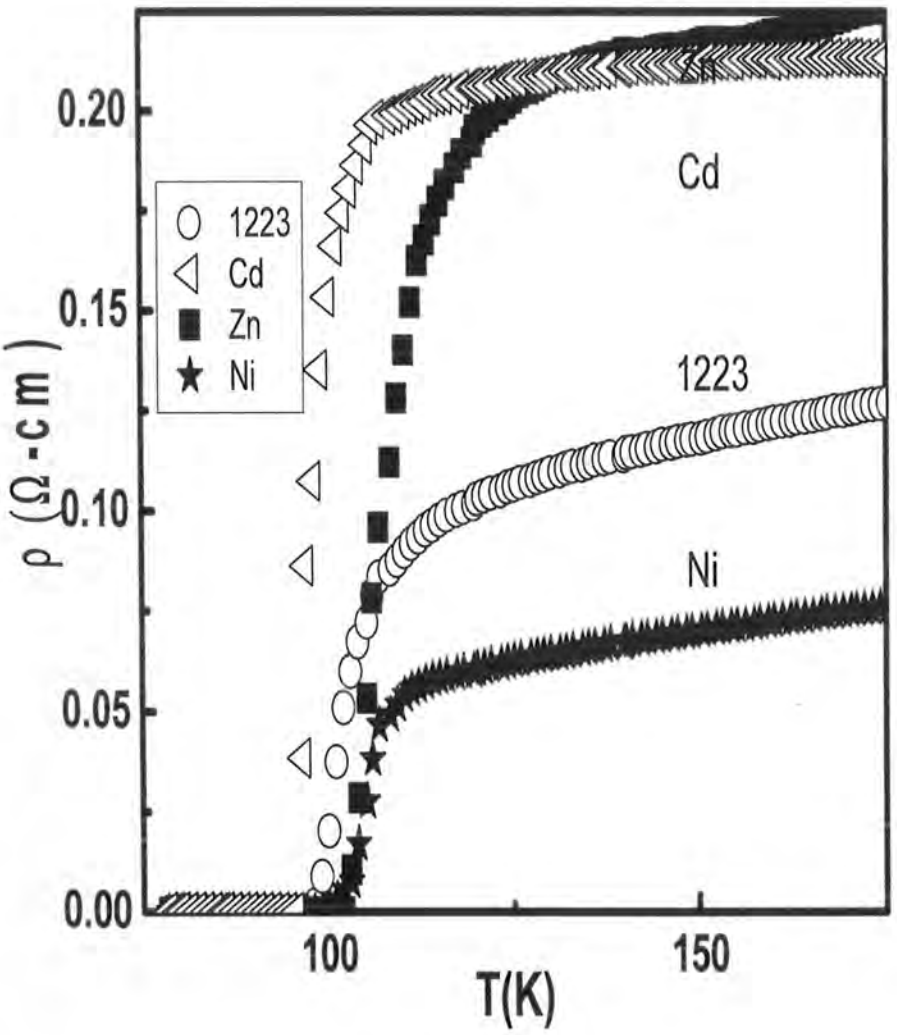

Fig.4.3. Resistivity versus temperature measurements of $Cu_{0.5}Tl_{0.5}Ba_2Ca_2Cu_3O_{10-\delta}$ and $Cu_{0.5}Tl_{0.5}Ba_2Ca_2Cu_{1.5}M_{1.5}O_{10-\delta}$ (M=Cd, Zn, Ni) samples

The ac-magnetic susceptibility of $Cu_{0.5}Tl_{0.5}Ba_2Ca_2Cu_{3-x}M_xO_{10-\delta}$ (M = Cd, Zn, Ni; x=0, 1.5) samples are shown in Fig. 4.4. The onset of diamagnetism in $Cu_{0.5}Tl_{0.5}Ba_2Ca_2Cu_{3-x}M_xO_{10-\delta}$

(M = Cd, Zn, Ni; x=0, 1.5) samples is around 113.6, 105, 105.2, 107.7K, Table 1. In Ni doped samples the magnitude of diamagnetism suppresses whereas it increases in Cd and Zn-doped samples.

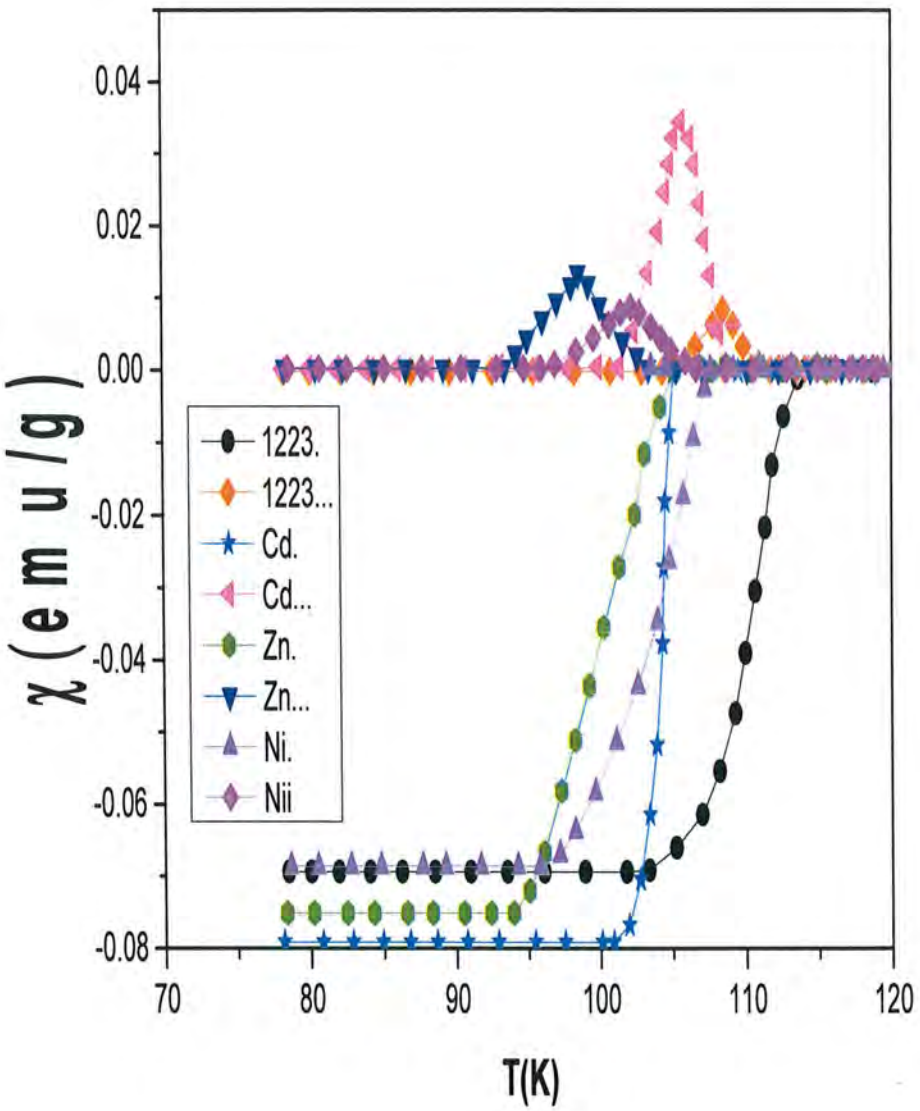

Fig.4.4. The AC susceptibility versus temperature measurements of $Cu_{0.5}Tl_{0.5}Ba_2Ca_2Cu_3O_{10-\delta}$ and $Cu_{0.5}Tl_{0.5}Ba_2Ca_2Cu_{1.5}M_{1.5}O_{10-\delta}$ (M=Cd, Zn, Ni) samples.

The FTIR absorption measurements of $Cu_{0.5}Tl_{0.5}Ba_2Ca_2Cu_{3-x}M_xO_{10-\delta}$ (M = Cd, Zn, Ni; x=0, 1.5) samples are shown in Fig.4.5. In these spectra the vibrational modes of of oxygen atoms $Cu_{0.5}Tl_{0.5}Ba_2Ca_2Cu_{3-x}M_xO_{10-\delta}$ (M = Cd, Zn, Ni; x=0, 1.5) unit cell are presented, which appeared between 400-700cm^{-1}. Three prominent absorption modes related to the vibrations of two apical oxygen atoms of type Tl-O_A-Cu(2), Cu(1)-O_A-Cu(2) and a CuO_2 planar oxygen modes are observed around 422-443, 520-543 and 575 cm^{-1}, respectively. The apical oxygen mode of type Tl-O_A-Cu(2) mode is hardened with the incorporation of samples (M = Cd, Zn, Ni) in the final compound, whereas the peak positions of other modes stays unchanged with doping of M atoms.

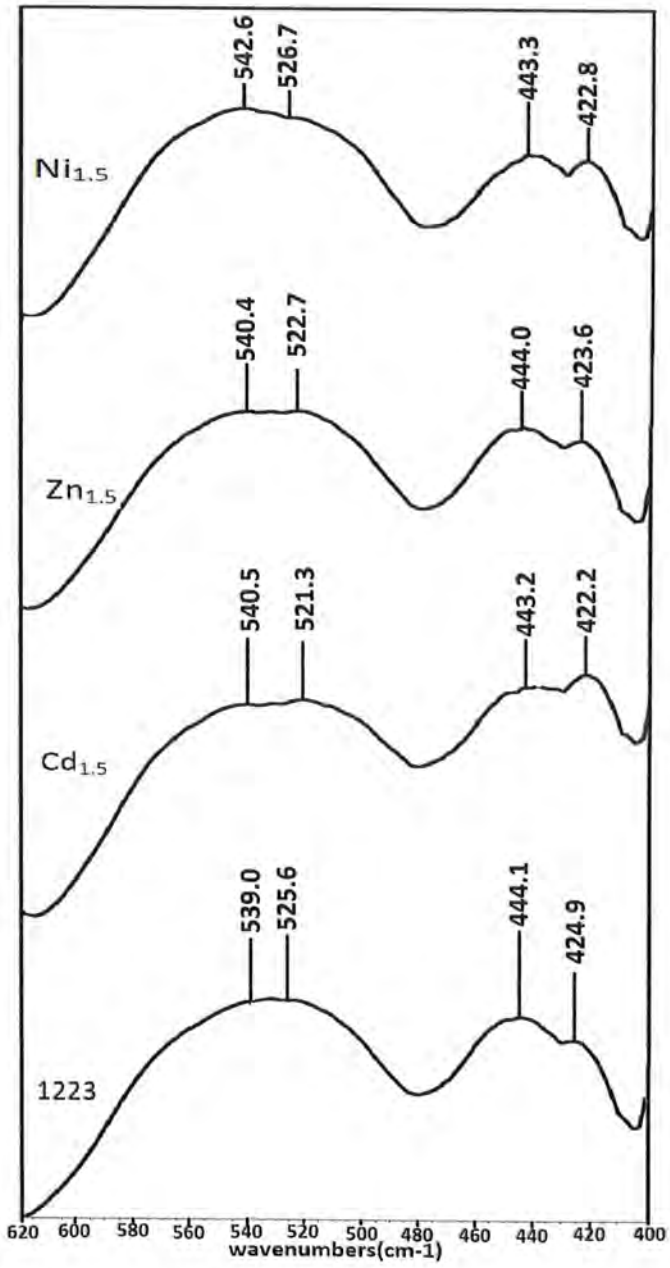

Fig.4.5. The FTIR absorbtion spectra of $Cu_{0.5}Tl_{0.5}Ba_2Ca_2Cu_3O_{10-\delta}$ and $Cu_{0.5}Tl_{0.5}Ba_2Ca_2Cu_{1.5}M_{1.5}O_{10-\delta}$ (M=Cd, Zn, Ni) samples.

The effect of doped M = Cd, Zn, Ni atoms on the dielectric properties of $Cu_{0.5}Tl_{0.5}Ba_2Ca_2Cu_{3-x}M_xO_{10-\delta}$ (x=0) samples has been investigated by taking their dielectric measurements from room temperature at 290K down to superconducting state around 80K.

4.3 Dielectric Properties of $Cu_{0.5}Tl_{0.5}Ba_2Ca_2Cu_{3-x}M_xO_{10-\delta}$ (M = Cd, Zn, Ni; x=0, 1.5) Samples:

In the low frequency range of 30-3000Hz only interfacial polarizations is possible in our $Cu_{0.5}Tl_{0.5}Ba_2Ca_2Cu_{3-x}M_xO_{10-\delta}$ (M = Cd, Zn, Ni; x=0, 1.5). Amongst the interfaces are:

(1) Interface between CuO_2/MnO_2 (M=Cd, Ni, Zn) planes and Cao layer.

(2) An interface between CuO_2/MnO_2 (M=Cd, Ni, Zn) planes and $Cu_{0.5}Tl_{0.5}Ba_2O_{4-\delta}$ charge reservior layer [28-29] .

The dielectric contribution of such interfaces becomes active at different frequencies [30]. The negative capacitance (NC) which imparts negative value to the dielectric constant ε' is typical feature of all $Cu_{0.5}Tl_{0.5}Ba_2Ca_2Cu_{3-x}M_xO_{10-\delta}$ (M = Cd, Zn, Ni; x=0, 1.5) samples. The most likely reasons for the negative dielectric constant is the difference in the effective masses of carriers in interfaces of $Cu_{0.5}Tl_{0.5}Ba_2Ca_2Cu_{3-x}M_xO_{10-\delta}$ (M = Cd, Zn, Ni; x=0, 1.5), in CuO_2 planes and metal contacts resulting into difference in the Fermi-levels. As a result, the Fermi-level of the ceramic samples is higher than the metal resulting into the flow of the carriers from the ceramic sample to metal and hence the negative capacitance and negative dielectric constant. The magnitude of negative value of the dielectric constant is observed to suppress with the increase of measurement temperature. The highest value of ε' are observed in $Cu_{0.5}Tl_{0.5}Ba_2Ca_2Cu_{3-x}M_xO_{10-\delta}$ (M = Cd, Zn, Ni; x=0, 1.5) samples in their superconducting state around 80K. The losses arising across the grain boundaries, localized defects and interfaces are reflected in the imaginary part of the dielectric constant (ε''); it is attenuation of energy across as the external electric field passes through the samples. Its value is positive and magnitude suppresses with increase in the applied frequency. The ratio of energy dissipated per radian to the energy stored determines the dielectric loss factor ($\tan\delta$) from which ac-conductivity and dielectric relaxation time is determined. In all our $Cu_{0.5}Tl_{0.5}Ba_2Ca_2Cu_{3-x}M_xO_{10-\delta}$ (M = Cd, Zn, Ni; x=0, 1.5) samples dielectric loss has been found to decrease with increase of measurement frequency.

The dielectric constant (ε') of $Cu_{0.5}Tl_{0.5}Ba_2Ca_2Cu_3O_{10-\delta}$ samples at different temperatures as a function of frequency is shown in Fig. 4.6a. The negative values of the

dielectric constant suppresses with the increase of measurement frequency at all temperatures. The larger decrease in the dielectric constant is witnessed below 100Hz showing that the higher frequencies begin to derive the material normal by inducing pair breaking effects. Moreover, the value of the dielectric constant also suppresses with the decrease of measurement temperature arising most likely from different amplitudes of oscillations of atoms of the interfaces at various temperatures and difference in effective masses of electrons. A systematic suppression in the real part of dielectric constant ε' is observed with decrease in the measurement temperature, however, the suppression of dielectric constant minimizes below the onset critical temperature showing that a portion of elementary excitation converted into boson fluid stays unaffected by applied low frequency.

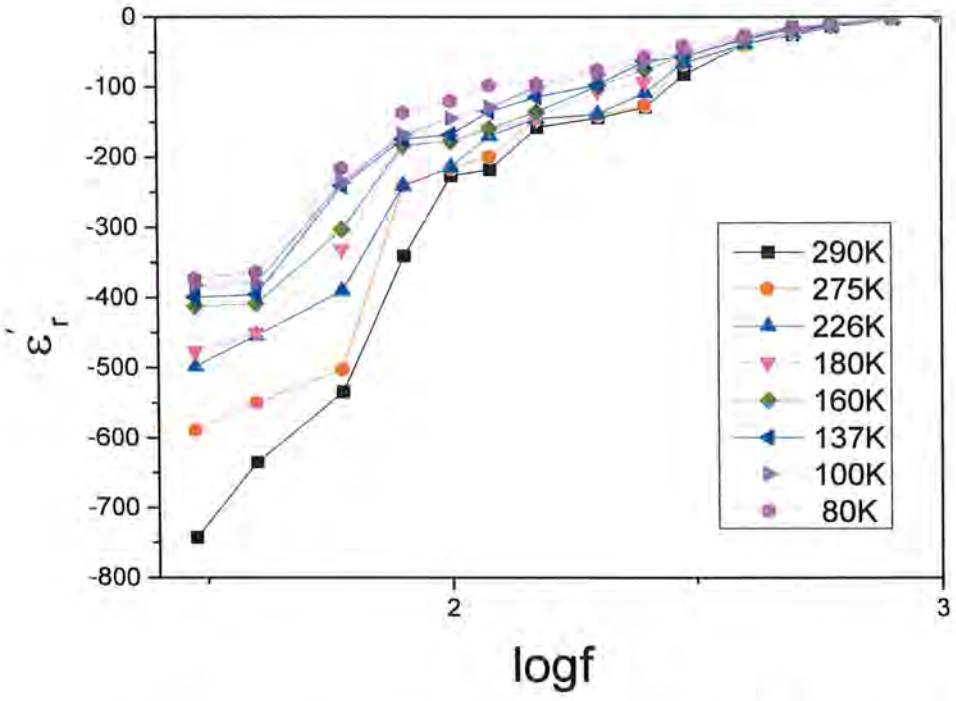

Fig. 4.6a: Variation of dielectric constant (ε') with frequency of $Cu_{0.5}Tl_{0.5}Ba_2Ca_2Cu_3O_{10-\delta}$ superconductors at different temperatures.

The real part of dielectric constant of $Cu_{0.5}Tl_{0.5}Ba_2Ca_2Cu_{3-x}M_xO_{10-\delta}$ (M = Cd, Zn, Ni; 1.5) samples is shown in Fig. 4.6(b,c,d). The negative value of the dielectric constant suppresses with the doping of Cd, Zn and Ni; the maximum decrease is observed in Cd-doped, then Ni-doped and finally in Zn-doped samples. One of the most likely reasons for the maximum

suppression of ε' in $Cu_{0.5}Tl_{0.5}Ba_2Ca_2Cu_{1.5}Cd_{1.5}O_{10-\delta}$ superconductors is difference in the masses of doped Cd and Cu atoms of CuO_2 planes that can induce anharmonic oscillation thereby suppressing the induced polarization by applied external electric field. The least suppression in Zn-doped $Cu_{0.5}Tl_{0.5}Ba_2Ca_2Cu_{1.5}Zn_{1.5}O_{10-\delta}$ superconductors is due to the small difference in mass with Cu-atoms and their spin less nature. Although the difference in the masses of Ni and Zn is the same but Ni-atoms have remnant spin which induces addition scattering thereby by inducing more suppression of dielectric constant.

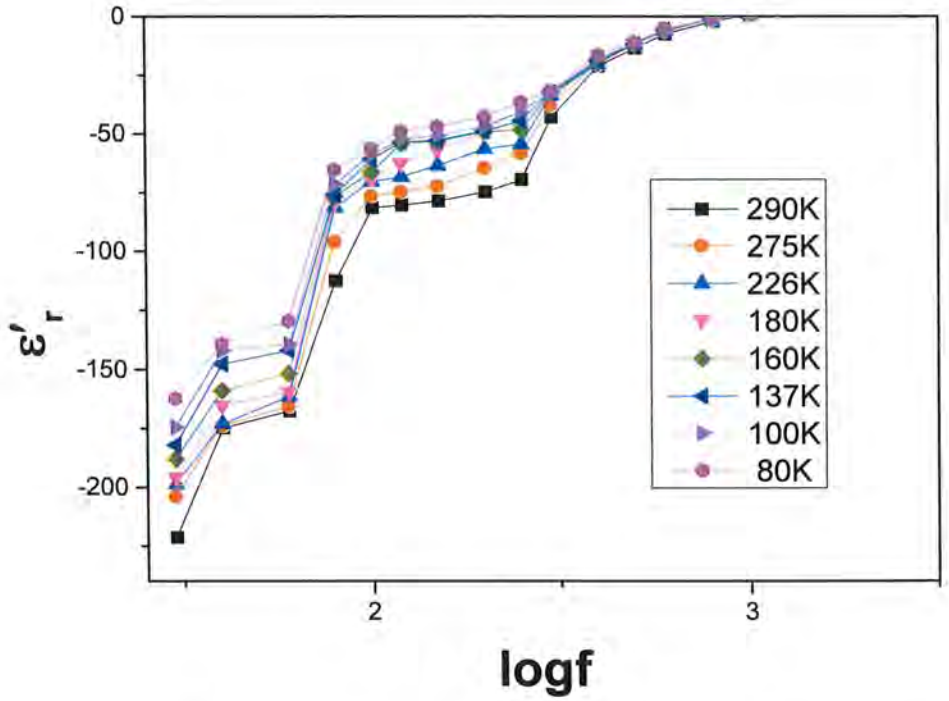

Fig. 4.6b: Variation of dielectric constant (ε') with frequency of $Cu_{0.5}Tl_{0.5}Ba_2Ca_2Cu_{1.5}Cd_{1.5}O_{10-\delta}$ superconductors at different temperatures.

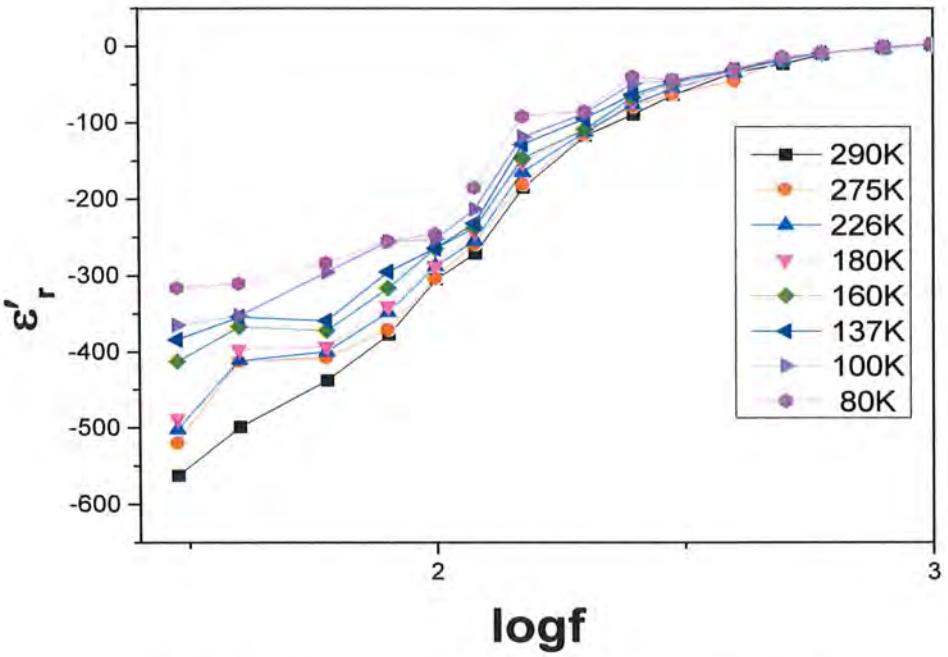

Fig. 4.6c: Variation of dielectric constant (ε') with frequency of $Cu_{0.5}Tl_{0.5}Ba_2Ca_2Cu_{1.5}Zn_{1.5}O_{10-\delta}$ superconductors at different temperatures.

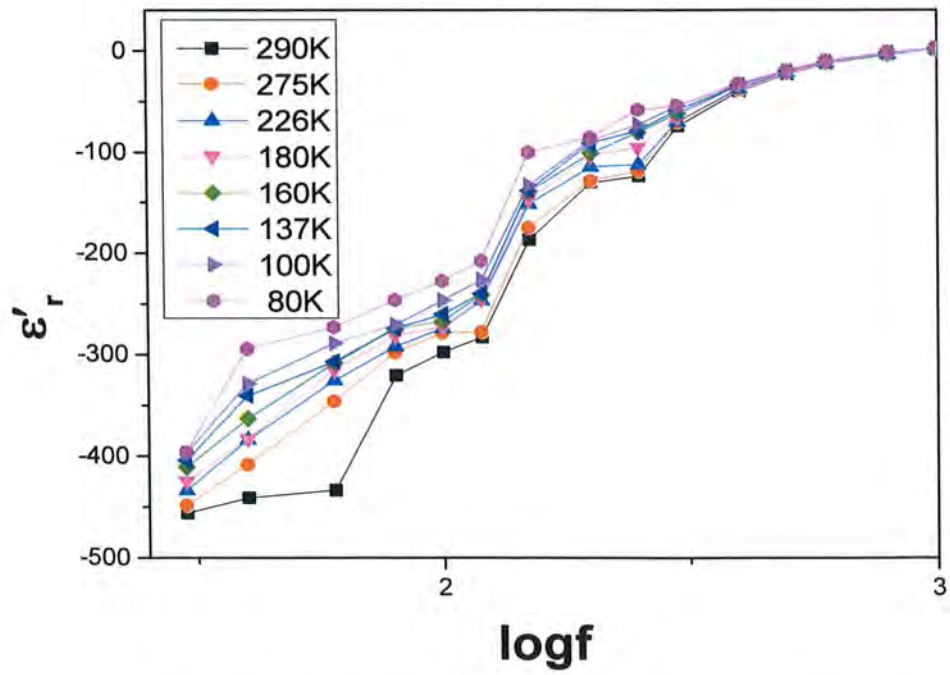

Fig.4.6d: Variations of dielectric constant (ε') with frequency of $Cu_{0.5}Tl_{0.5}Ba_2Ca_2Cu_{1.5}Ni_{1.5}O_{10-\delta}$ superconductors at different temperatures.

The imaginary part of dielectric constant ε'' of $Cu_{0.5}Tl_{0.5}Ba_2Ca_2Cu_{3-x}M_xO_{10-\delta}$ (M = Cd, Zn, Ni; x=0, 1.5) samples is shown in Fig. 4.7(a,b,c,d); it is related to the losses across the interfaces. The values of ε'' suppresses with the increase of applied field in all samples. This shows that the wave vector of applied electric filed matches with the wave vector of interfaces at low frequencies. The maximum values of ε'' is observed in in un-doped $Cu_{0.5}Tl_{0.5}Ba_2Ca_2Cu_3O_{10-\delta}$ sampels then in Ni-doped, Zn-doped and finally in Cd-doped samples. The samples with higher values of ε'' have also shown the higher values of real part of dielectric constant ε' manifesting that losses are associated with the magnitude of the polarization in the samples. Despite having the same difference in masses with the Cu atoms, the value of ε'' observed in $Cu_{0.5}Tl_{0.5}Ba_2Ca_2Cu_{1.5}Ni_{1.5}O_{10-\delta}$ samples is higher than that of Zn-doped $Cu_{0.5}Tl_{0.5}Ba_2Ca_2Cu_{1.5}Zn_{1.5}O_{10-\delta}$ samples, arising most likely from the additional spin scattering in Ni-doped samples. Moreover, in the superconducting state there is a larger increase observed in ε' and ε'' is in un-doped $Cu_{0.5}Tl_{0.5}Ba_2Ca_2Cu_3O_{10-\delta}$samples in comparison with doped $Cu_{0.5}Tl_{0.5}Ba_2Ca_2Cu_{3-x}M_xO_{10-\delta}$ (M = Cd, Zn, Ni; x=1.5) samples that shows that the pristine samples have more superconductor volume fraction than in Ca, Zn and Ni-doped samples.

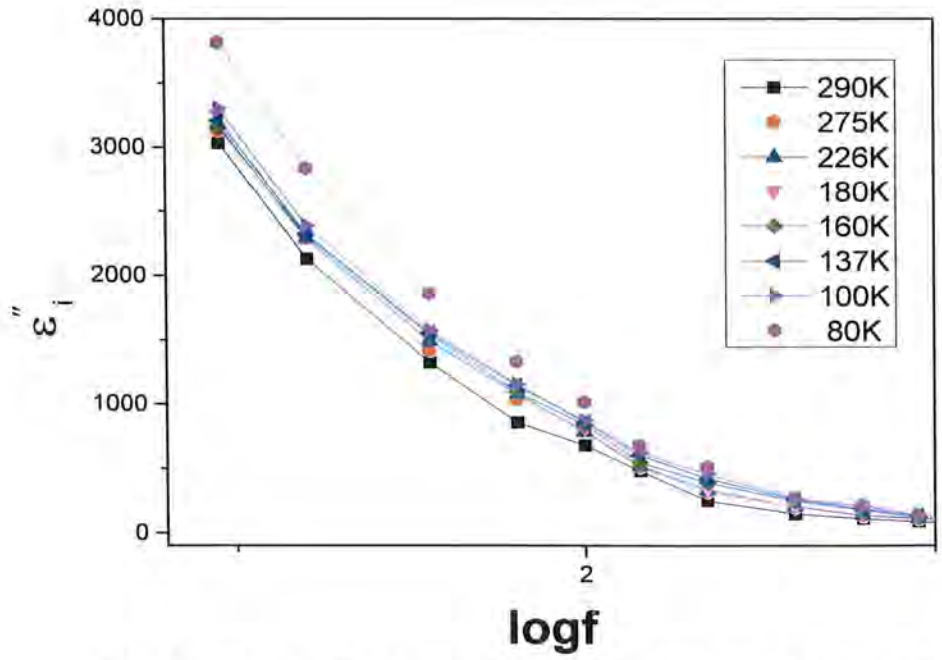

Fig. 4.7a: Variation of imaginary dielectric constant (ε'') with frequency of $Cu_{0.5}Tl_{0.5}Ba_2Ca_2Cu_3O_{10-\delta}$ superconductor at different temperatures.

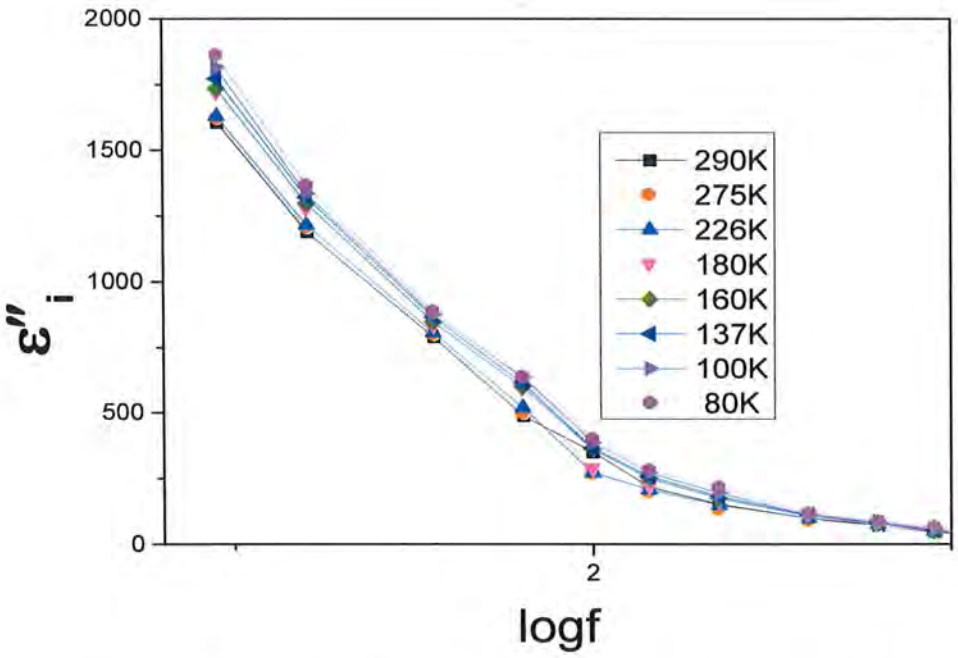

Fig. 4.7b: Variation of imaginary dielectric constant ($\varepsilon^{//}$) with frequency of $Cu_{0.5}Tl_{0.5}Ba_2Ca_2Cu_{1.5}Cd_{1.5}O_{10-\delta}$ superconductor at different temperatures.

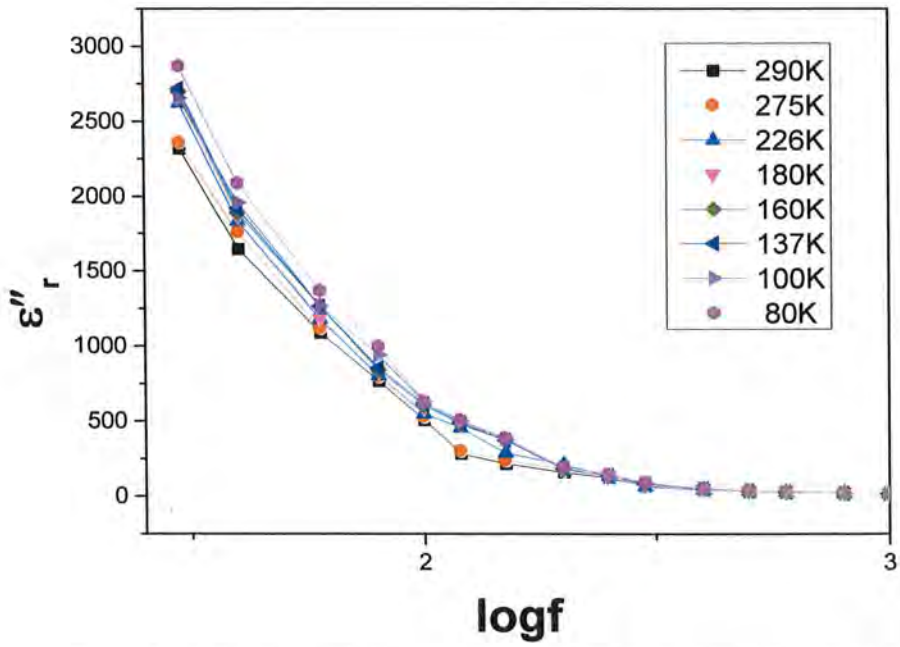

Fig. 4.7c: Variation of imaginary dielectric constant ($\varepsilon^{//}$) with frequency of $Cu_{0.5}Tl_{0.5}Ba_2Ca_2Cu_{1.5}Zn_{1.5}O_{10-\delta}$ superconductor at different temperature.

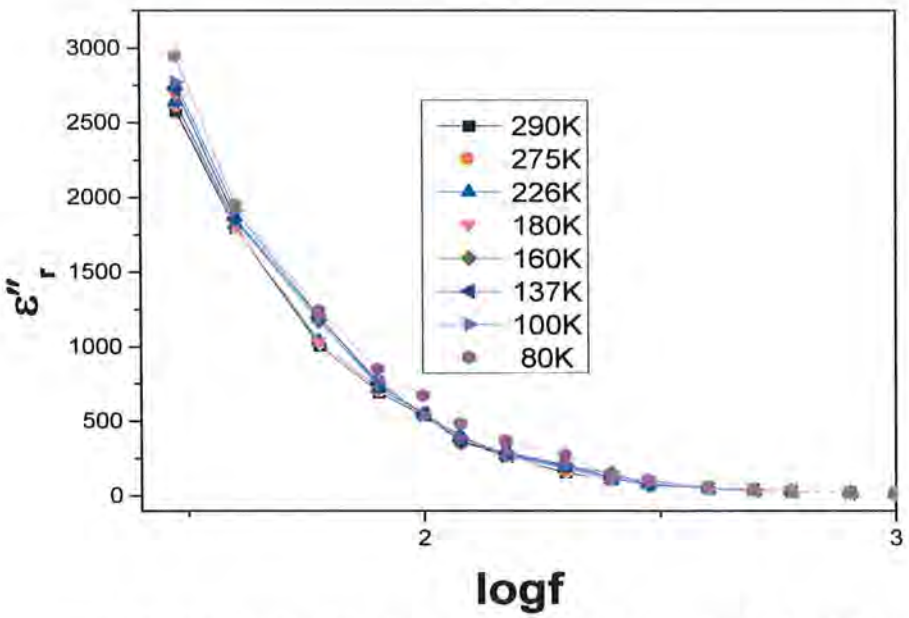

Fig. 4.7d: Variation of imaginary dielectric constant ($\varepsilon^{//}$) with frequency of $Cu_{0.5}Tl_{0.5}Ba_2Ca_2Cu_{1.5}Ni_{1.5}O_{10-\delta}$ superconductor at different temperatures.

The dielectric loss factor (tanδ) $Cu_{0.5}Tl_{0.5}Ba_2Ca_2Cu_{3-x}M_xO_{10-\delta}$ (M = Cd, Zn, Ni; x=0, 1.5) samples is shown in Fig. 4.8(a,b,c,d). Its systematically suppresses with the increase of measurement frequency and increases with the suppression of measurement temperature. A crossover from a negative to a positive value of tanδ occurs around 900Hz in all $Cu_{0.5}Tl_{0.5}Ba_2Ca_2Cu_{3-x}M_xO_{10-\delta}$ (M = Cd, Zn, Ni; x=0, 1.5) samples that most likely arises from the activation of different interfacial polarization at different frequencies. We have suggested below 1000Hz $CuO_2/Cu_{0.5}Tl_{0.5}Ba_2O_{4-\delta}$ interfaces and at 1000Hz and above the CuO_2/CaO interfacial effects are activated. The activation of these interfacial effects are prone to matching of wave vectors associated with the various interfaces and applied electric field. It can be seen from Fig. 4.8(a,b,c,d) that the losses in all the doped samples are higher in comparison with pristine un-doped sample.

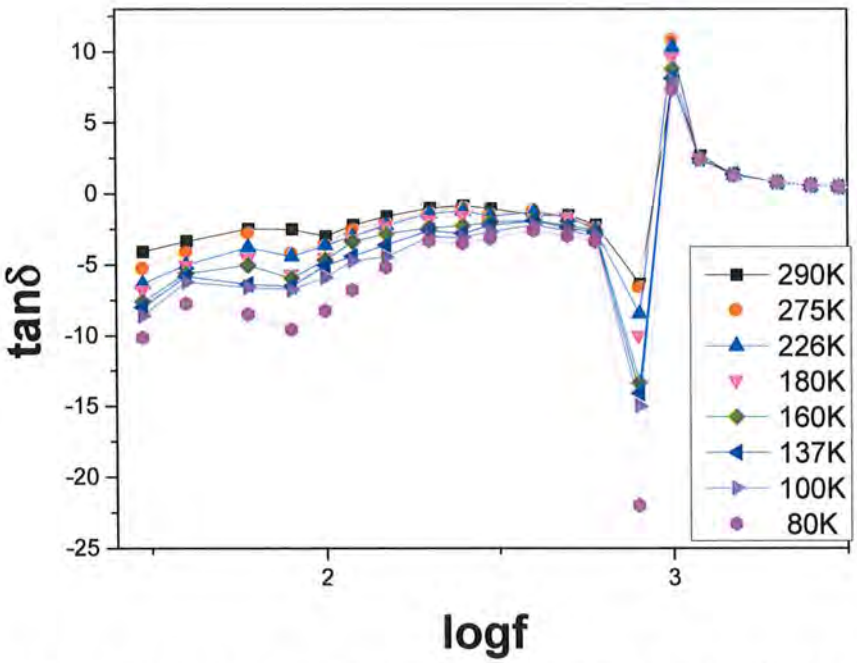

Fig. 4.8a: Dielectric loss (tanδ) versus frequency of $Cu_{0.5}Tl_{0.5}Ba_2Ca_2Cu_3O_{10-\delta}$ superconductors at different temperatures.

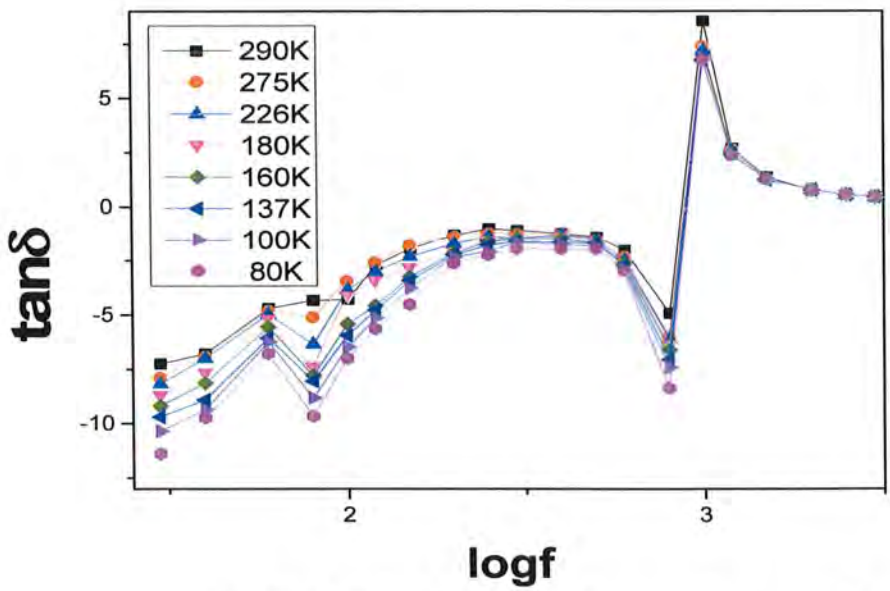

Fig. 4.8b: Dielectric loss (tanδ) versus frequency of $Cu_{0.5}Tl_{0.5}Ba_2Ca_2Cu_{1.5}Cd_{1.5}O_{10-\delta}$ superconductors at different temperatures.

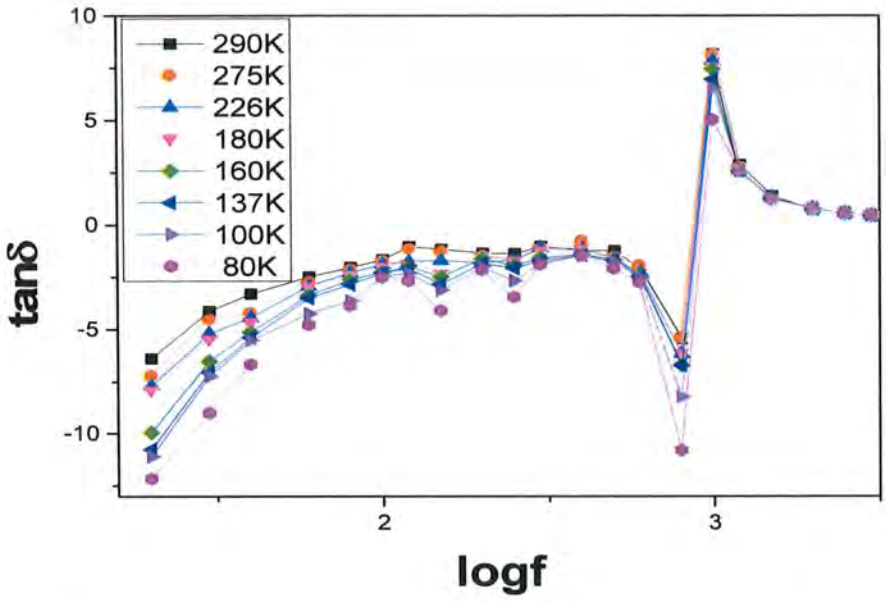

Fig. 4.8c: Dielectric loss (tanδ) versus frequency of $Cu_{0.5}Tl_{0.5}Ba_2Ca_2Cu_{1.5}Zn_{1.5}O_{10-\delta}$ superconductor at different temperatures.

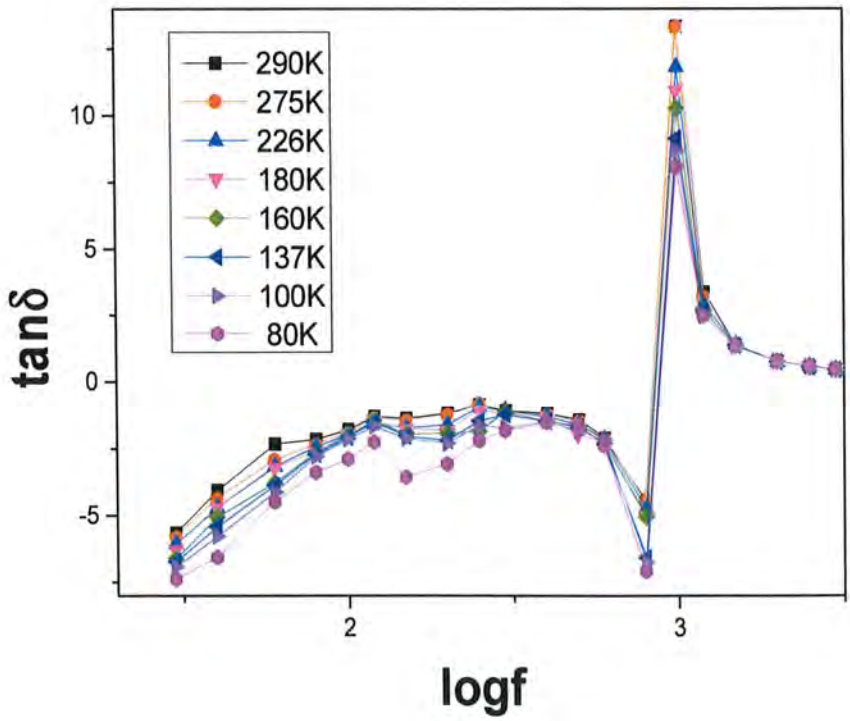

Fig. 4.8d: Dielectric loss (tanδ) versus frequency of $Cu_{0.5}Tl_{0.5}Ba_2Ca_2Cu_{1.5}Ni_{1.5}O_{10-\delta}$ superconductors at different temperatures.

The ac-conductivity (σ_{ac}) of $Cu_{0.5}Tl_{0.5}Ba_2Ca_2Cu_{3-x}M_xO_{10-\delta}$ (M = Cd, Zn, Ni; x=0, 1.5) samples is shown in Fig.4.9(a,b,c,d). A systematic suppression of σ_{ac} with the increase of measurement frequency is typical feature of all the samples. Moreover, σ_{ac} increases with the suppression of measurement temperature. A jump of enhancement ac-conductivity could be witnessed in pristine $Cu_{0.5}Tl_{0.5}Ba_2Ca_2Cu_3O_{10-\delta}$ samples. The magnitude of this enhanced conductivity is suppressed in Zn and Ni-doped samples where as it is altogether minimized in Cd-doped samples. The enhancement in the ac-conductivity most likely arises from the superconducting state of the system as the $T_c(R=0)$ of $Cu_{0.5}Tl_{0.5}Ba_2Ca_2Cu_3O_{10-\delta}$ samples is 105.6K. This jump in the ac-conductivity from the normal to the superconducting state determines the strength of the superconductivity and magnitude of diamagnetism in the final compound. The smallest ac-conductivity gap between the normal and superconducting state in the Cd-doped $Cu_{0.5}Tl_{0.5}Ba_2Ca_2Cu_{1.5}Cd_{1.5}O_{10-\delta}$ samples shows that doped Cd-atoms generate the an-harmonic oscillations that in turn produce the pair breaking effects and suppress the superconducting volume fraction. These studies have shown that electron phono-intraction is essential for the mechanism of high T_c superconductivity in oxide superconductors.

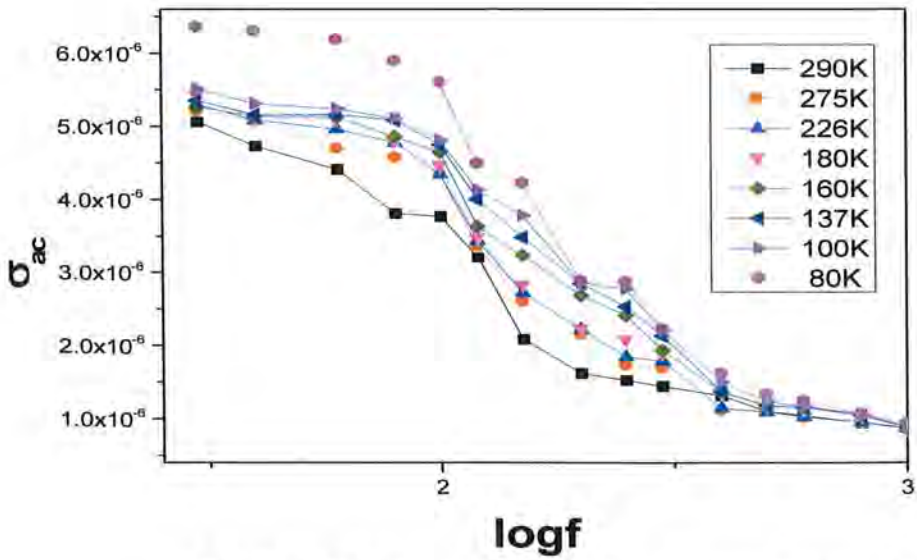

Fig. 4.9a: Plot of ac-conductivity (σ_{ac}) versus frequency of $Cu_{0.5}Tl_{0.5}Ba_2Ca_2Cu_3O_{10-\delta}$ superconductors at different temperatures.

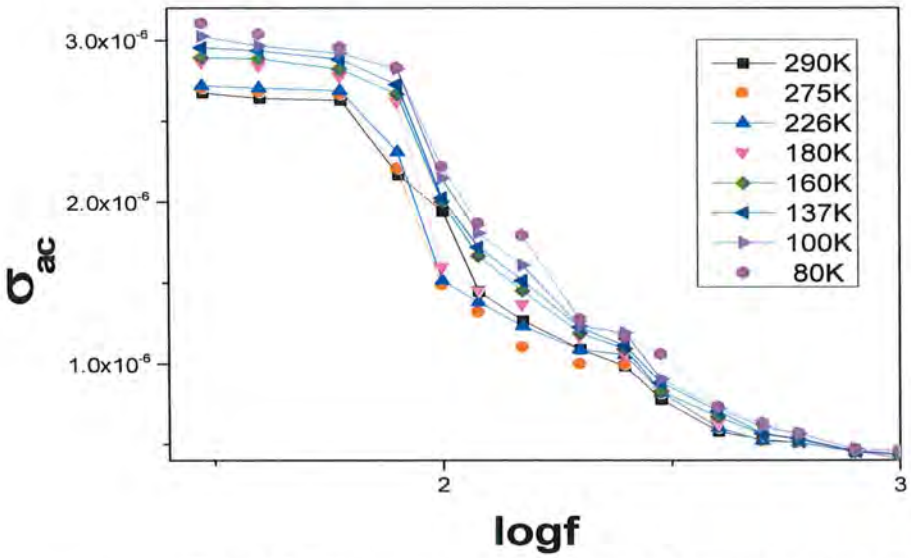

Fig. 4.9b: Plot of ac-conductivity (σ_{ac}) versus frequency of $Cu_{0.5}Tl_{0.5}Ba_2Ca_2Cu_{1.5}Cd_{1.5}O_{10-\delta}$ superconductors at different temperatures.

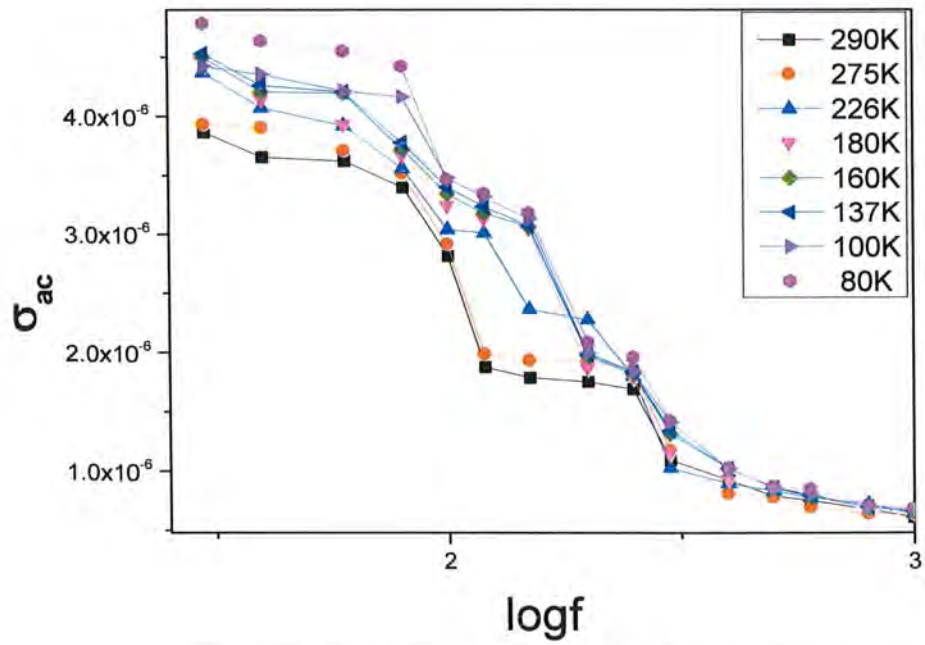

Fig. 4.9c: Plot of ac-conductivity (σ_{ac}) versus frequency of $Cu_{0.5}Tl_{0.5}Ba_2Ca_2Cu_{1.5}Zn_{1.5}O_{10-\delta}$ superconductors at different temperatures.

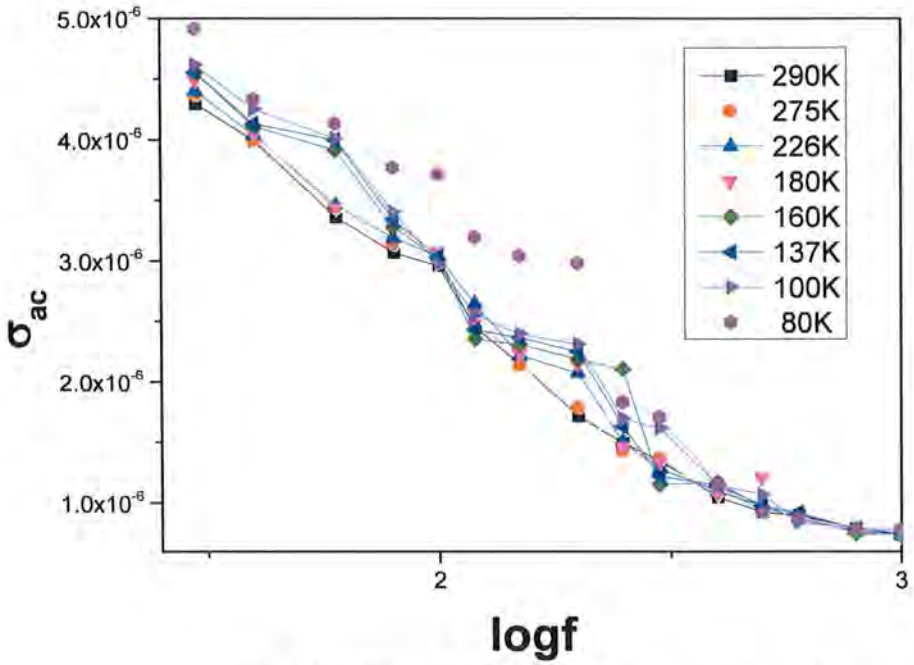

Fig. 4.9d: Plot of ac-conductivity (σ_{ac}) versus frequency of $Cu_{0.5}Tl_{0.5}Ba_2Ca_2Cu_{1.5}Ni_{1.5}O_{10-\delta}$ superconductors at different temperatures.

4.4 Conclusions:

1. We have successfully synthesized $Cu_{0.5}Tl_{0.5}Ba_2Ca_2Cu_{3-x}M_xO_{10-\delta}$ (M = Cd, Zn, Ni; x=0, 1.5) samples and studied their low frequency dielectric measurements (ε' & ε'') using multi-frequency LCR Meter from 30Hz to 3100Hz.

2. $Cu_{0.5}Tl_{0.5}Ba_2Ca_2Cu_{3-x}M_xO_{10-\delta}$ (M = Cd, Zn, Ni; x=0, 1.5) samples have shown orthorhombic crystal structure with increase in the length of a-axis length and suppression of the b & c-axes length with the incorporation of Cd, Zn, Ni in the final compound. The onset temperature of the superconductivity and Tc(R=0) suppress with the doping of Cd whereas its values increase with the incorporation of Zn and Ni in the final compound. The onset temperature of superconductivity observed in the ac-susceptibility measurements suppresses in all doped sample, however, the maximum suppression is observed in Cd-doped samples. The apical oxygen phonon mode of type Tl-O_A-Cu(2) mode is hardened with the doping of

Cd, Zn, Ni in the final compound, however, the peak positions of other modes stays at the usual position as observed in un-doped samples.

3. The real and imaginary parts of the dielectric constants of $Cu_{0.5}Tl_{0.5}Ba_2Ca_2Cu_{3-x}M_xO_{10-\delta}$ (M = Cd, Zn, Ni; 1.5) samples have been found to suppress with the increase of applied measurement frequency, however, the absolute value of ε' and ε'' increase with the lowering of measurement temperatures.

4. The magnitude of real ε' and imaginary parts ε'' of dielectric constants decrease with the doping of Cd, Zn, Ni; the maximum decrease is observed in Cd-doped, then Ni-doped and finally in Zn-doped samples. A maximum suppression in the values of real and imaginary parts of dielectric constants in Cd-doped samples is suggested to be arising from the generation of an-harmonic oscillations in the CuO_2/CdO_2 planes due to the difference in the masses Cu and Cd atoms. These an-harmonic oscillations most likely suppress the density of essential phonons required for electron-phonon interactions thereby promoting suppression in the population of Cooper-pairs and hence the dielctric constants.

5. A novel shift in dielectric loss (tanδ) from the negative to the positive values has been observed in the frequency region between 800Hz and 1000Hz in all $Cu_{0.5}Tl_{0.5}Ba_2Ca_2Cu_{3-x}M_xO_{10-\delta}$ (M = Cd, Zn, Ni; 1.5) samples. We attribute this to be arising from the interactions of applied frequency with low K-values $CuO_2/Cu_{0.5}Tl_{0.5}Ba_2O_{4-\delta}$ interfaces activated below1000Hz and higher K-values CuO_2/CaO interfaces are activated above 1000Hz.

6. A jump of enhancement ac-conductivity in $Cu_{0.5}Tl_{0.5}Ba_2Ca_2Cu_3O_{10-\delta}$ samples is observed 80K, the magnitude of it suppressed in Zn and Ni-doped samples where as it becomes very small in Cd-doped samples. We attribute this to the generation of an-harmonic oscillations which the pair breaking effects consequently suppressing the extra or excess ac-conductivity of $Cu_{0.5}Tl_{0.5}Ba_2Ca_2Cu_{1.5}Cd_{1.5}O_{10-\delta}$ samples.

References:

[1] Xiao, G., Cieplak, M.Z., Gavrin, A., Streitz, F.H., Bakhshai, A., Chien, C.L.: Phys. Rev. Lett., 60(1988) 1446.

[2] A. Raza, S. H. Safeer, N. A. Khan : J. Superconductor and Nov. Mag., (2016)

[3] Kandyel, E., Sekkina, M.A., Dawoud, M.A.T., Bohnam, M.Y.: Solid State Commun. 135 (2005) 214–219.

[4] Tominoto, K., Terasaki, I., Rykov, A.I., Mimura, T., Tajima, S.: Phys. Rev. B, 60(1999) 114.

[5] Hidekazu Mukuda, Sunao Shimizu, Akira Iyo, and Yoshio Kitaoka: J. Phys. Soc. Jpn. 81 (2012).

[6] Fukuzumi,Y.,etal.:Phys.Rev.Lett.76 (1996) 684.

[7] C. W. Chu, L. Z. Deng and B. Lv.: Physica C, 514(2015)290-313.

[8] . Hudson, E.W., Lang, K.M., Madhavan, V., Pan, S.H., Eisak, H., Uchida, S., Davis, J.C.: Nature, 411(2001)920

[9] Alloul, H., Mendels, P., Casalta, H., Marucco, J.F., Arabski, J.: Phys. Rev. Lett.67,(1991) 3140.

[10] Vieira,V.N.,Pureur,P.,Schaf,J.:Phys. Rev. B66,(2002) 224506.

[11] E. W. Hudson, K. M. Lang, V. Madhavan, S. H. Pan, H. Eisaki, S. Uchida, J. C. Davis: Nature,411(2001) 920-924.

[12] Akoshima, M., Noji, T., Ono, Y., Koike, Y.: Phys. Rev. B57,(1998) 7491.

[13] Kuo, Y.K., Schneider, C.W., Skove, M.J., Nevitt, M.V., Tessema, G.X., McGee, J.J.: Phys. Rev. B 56 (1997) 6201.

[14] Hanaki,Y.,Ando,Y.,Ono,S.,Takeya,J.:Phys.Rev.B64,(2001) 172514

[15] Tallon, J.L., Berhard, C., Williams, G.V.M., Loram, J.W.: Phys. Rev. Lett. 79(1997) 5294.

[16] Kakinuma, N., Ono, Y., Koike, Y.: Phys. Rev. B 59 (1999) 1491.

[17] Kaplan, I.G., Soullard, J., Hernandez-Cobos, J.: Phys. Rev. B 65(2002) 214509.

[18] Y. F. Guo, Y. G. Shi, S. Yu, A. A. Belik, Y. Matsushita, M. Tanaka, Y. Katsuya, K. Kobayashi, I. Nowik,6I. Felner, V. P. S. Awana, K. Yamaura,and E. Takayama-Muromachi: Physical Review 82(2010).

[19] Nawazish A. K., M. Mumtaz, A. A. Khurrum,:J. of Appli. Physics 104 (2008) 033916.
[20] M. Mumtaz, L. Ali, S. Azeem, S. Ullah, G. Hussain, M.W. Rabbani, A. Jabbar, K. Nadeem: J. Advance Ceramics, 5 (2016)160.
[21] W. Kim, Ch. Ahn, J. Kima, T. Song, :App. Physics Lett.80 (2002) 21.
[22] M. Mumtaz, M. Kamran, K. Nadeem, Abdul Jabbar, N.A. Khan, A. Saleem, S. T. Hussain: Low temperature Physics, 39 (2013) 807.
[23] M. Mumtaz, Rahim M, N.A. Khan, K. Nadeem, K. Shehzad: Ceramic International, 39 (2013) 9592.
[24] P. Ben-Ishai, E. Sedar, Y. D. Feldman, M.Weger: J. of Superconductivity,18(4),(2005)
[25] S. Çavdar, H. Koralay, N.Tuguloglu, A. Gunen : Sup. Sci and Tec. 18 (2005)1204.
[26] X. Xu, Z. jiao, M. Fu, L. Fing, K. Xu, R.Zuo, X.Chen; Pysica C, 417 (2005)

[27] R.K. Nkum, M.O. Gyekye, F. Boakye: Solid State Commun. 122 (2002)569.

[28] N. A. Khan, G. Husnain, K. Sabeeh : J. Phys. Chem. Solids 67 (2006) 1841-1849.
[29] H. Ihara, Tokiwa K., Tanaka K.:Physics C, 282-287 (1997) 957-958.

[30] S. B. Ocak, A. B. Selcuk, S. B. Bayram, A. Ozbay: Journal of Optoelectronic and Advanced Materials,17(2015).